Computational Aspects of Discrete Minimal Surfaces

Konrad Polthier

Sept. 10, 2002

In differential geometry the study of smooth submanifolds with distinguished curvature properties has a long history and belongs to the central themes of this field. Modern work on smooth submanifolds, and on surfaces in particular, relies heavily on geometric and analytic machinery which has evolved over hundreds of years. However, non-smooth surfaces are also natural mathematical objects, even though there is less machinery available for studying them. Consider, for example, the pioneering work on polyhedral surfaces by the Russian school around Alexandrov [1], or Gromov's approach of doing geometry using only a set with a measure and a measurable distance function [10]. Also in other fields, for example in computer graphics and numerics, we nowadays encounter a strong need for a discrete differential geometry of arbitrary meshes.

These tutorial notes introduce the theory and computation of discrete minimal surfaces which are characterized by variational properties, and are based on a part of the authors Habilitationsschrift [27]. In Section 1 we introduce simplicial surfaces and their function spaces. Laplace-Beltrami harmonic maps and the solution of the discrete Cauchy-Riemann equations are introduced on simplicial surfaces in Section 2. These maps are the basis for an interative algorithm to compute discrete minimal and constant mean curvature surfaces which is discussed in Section 3. There we define the discrete mean curvature operator, derive the associate family of discrete minimal surfaces in terms of conforming and non-conforming triangles meshes, and present some recently discovered complete discrete surfaces, the family of discrete catenoids and helicoids.

1
Introduction to Polyhedral Meshes

Polyhedral meshes belong to the most basic structures for the representation of geometric shapes not only in numerics and computer graphics. Especially the finiteness of the set of vertices and of their combinatorial relation makes them an ideal tool to reduce infinite dimensional problems to finite problems. In this section we will review the basic combinatorial and topological definitions and state some of their differential geometric properties.

In practice, a variety of different triangle and other polyhedral meshes are used. In this introduction we restrict ourselves to simplicial complexes, or conforming meshes, where two polygons must either be disjoint or have a common vertex or a common edge. Or for short, a polygon is not allowed to contain a vertex of another polygon in the interior of one of its edges. This restriction avoids discontinuity problems in the shape, so-called hanging nodes. Further, we restrict our discussion to piecewise linear meshes although many concepts extend to meshes with piecewise higher order polynomial order. Often it is too restrictive to work solely in the space of conforming triangulations, and, in later chapters, we will enlarge the function space to include discontinuous, non-conforming meshes as well.

In many situations a property of a polyhedral surface can be associated to depend either on the geometric shape or on the combinatorial respectively topological properties of the mesh. Therefore, it

is important to distinguish between the topology of a mesh and its geometric shape which is determined by the geometric position of the vertices. For example, assume that all points of a compact surface are collapsed to a single geometric position, then we would still like to derive the topological genus from the combinatorial properties of the surface. This forces us to introduce slightly more abstract definitions of polyhedral surfaces.

Introductions to polyhedral manifolds are given in most books on algebraic topology, for example by Munkres [22], in the book by Ziegler [38] on combinatorial aspects of polytopes, or by Bloch [2] on topological and differential geometric problems. But note, there are slight differences depending on the purpose. The standard approach in topology introduces simplices and simplicial complexes as embeddings into Euclidean space while we allow immersions with self-intersections. Good sources of applications of polyhedral manifolds to problems in differential geometry are also the books by A.D. Alexandrov and Zalgaller [1] and Reshetnyak [35].

1.1 Simplicial Complexes

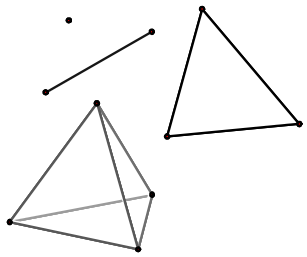

Low dimensional simplices.

We begin the introduction of polyhedral surfaces with a combinatorial point of view, that means, for the moment we do not care about the specific nature of points but consider them as abstract entities. In the combinatorial setup the most basic entities of polyhedral shapes are points, line segments, triangles, tetrahedrons, and their higher dimensional analogues, called simplices:

Definition 1 *Let* $\mathfrak{V} = \{\mathfrak{v}_0, .., \mathfrak{v}_m\}$ *be a finite set of* $m+1$ *abstract points. The (unordered) set* $[\mathfrak{v}_0, .., \mathfrak{v}_m]$ *is called a* combinatorial $m-$simplex*, or short, a* combinatorial simplex*. The number* m *is called the* dimension of the simplex*.*

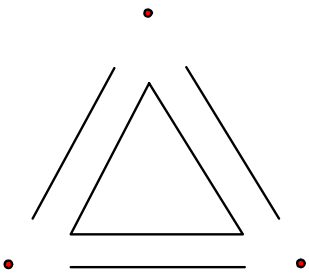

Faces of a triangle.

Definition 2 *A* face *f of a simplex $\sigma = [\mathfrak{v}_0, .., \mathfrak{v}_m]$ is a simplex determined by a non-empty subset of $\{\mathfrak{v}_0, .., \mathfrak{v}_m\}$. A $k-$face has $k+1$ points. A* proper *face is any face different from σ.*

For example, a $0-$simplex is a combinatorial point, a $1-$simplex is a line segment, a $2-$simplex is a triangle, and a $3-$simplex is a tetrahedron. There exist seven faces of a triangle $[\mathfrak{v}_0, \mathfrak{v}_1, \mathfrak{v}_2]$: the triangle itself $[\mathfrak{v}_0, \mathfrak{v}_1, \mathfrak{v}_2]$, its three edges $[\mathfrak{v}_0, \mathfrak{v}_1]$, $[\mathfrak{v}_1, \mathfrak{v}_2]$, $[\mathfrak{v}_2, \mathfrak{v}_0]$ and its three points $[\mathfrak{v}_0]$, $[\mathfrak{v}_1]$, $[\mathfrak{v}_2]$, where the last six faces are proper. A $0-$simplex has no proper face.

To perform the transition from combinatorics to geometry, we use the so-called standard simplex which serves as geometric representative associated to each combinatorial simplex:

Definition 3 *The* standard simplex $\Delta^m \subset \mathbb{R}^{m+1}$ *is the convex hull of the endpoints* $\{e_0, .., e_m\}$ *of the unit basis vectors in* $\mathbb{R}^m$ *which are given by* $e_i = (0, .., 0, 1, 0, .., 0)$. *Formally,*

$$\Delta^m = \left\{ \sum_{i=0}^{m} \lambda_i e_i \;\middle|\; 0 \leq \lambda_i \leq 1,\ \sum_{i=0}^{m} \lambda_i = 1 \right\}.$$

Note, the standard simplex not only is a set of points but includes the "interior" points. For example, the standard triangle Δ^2 in $\mathbb{R}^3$ is the planar triangle spanned by the three points $(1, 0, 0)$, $(0, 1, 0)$, $(0, 0, 1)$. Nevertheless, the standard simplex is simply a technical term. It provides the ground to formulate that any set of $m + 1$ points in a Euclidean space $\mathbb{R}^n$ defines a geometric simplex:

Definition 4 *A* geometric simplex $\sigma = [p_o, .., p_m]$ *is a set* $V = \{p_o, .., p_m\}$ *of* $m+1$ *points in* $\mathbb{R}^n$, *where* n *might be different from* m, *together with an affine map*

$$\varphi : \Delta^m \to convHull(p_0, .., p_m)$$
$$\varphi(e_i) = p_i.$$

The number m *is called the* dimension of the simplex.

The difference between an abstract and a geometric simplex is the existence of the geometric realization provided by the map φ, that means, the embedding of the simplex in a vector space.

Definition 5 *Let* $\mathfrak{V} = \{\mathfrak{v}_1, \mathfrak{v}_2, ..\}$ *be a set of abstract points. Then an* abstract simplicial complex K *is a set of simplices* S *formed by finite subsets of* $\mathfrak{V}$ *such that if* $\sigma \in S$ *is a simplex, then every subset* $\tau \subset \sigma$ *is also a simplex of* K.
If two, or more, simplices of K *share a common face, they are called* adjacent *or* neighbours. *The* boundary *of* K *is formed by any proper face that belongs to only one simplex, and its faces.*

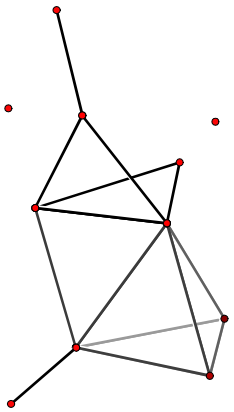

Simplicial Complex.

The simplicial complex K formally represents the connectivity of a mesh, and its simplices represent the points, edges, triangles, and higher dimensional simplices. The number of points in a complex may be infinite. By associating the set of abstract points with geometric

points in some $\mathbb{R}^n$ we obtain a geometric shape consisting of piecewise flat simplices. Note, the following definition does not require an embedding but allows that the geometric realization may have self-intersections. By allowing immersions this definition is non-standard in the sense of algebraic topology which usually requires embeddings.

Definition 6 *A* simplicial complex (K, V) *of an abstract simplicial complex K is a geometric realization uniquely given by*

1. *a set of geometric points $V = \{p_1, p_2, ..\} \subset \mathbb{R}^n$ with a bijection*

$$\Phi : \mathfrak{V} \to V$$
$$\mathfrak{v}_i \to p_i.$$

2. *for each $k-$simplex $\sigma = [p_{i_0}, .., p_{i_k}]$ an affine map from the standard simplex*

$$\varphi : \Delta^k \to convHull(p_{i_0}, .., p_{i_k})$$
$$\varphi(e_j) = p_{i_j}.$$

The above definitions ensure a strict separation between the combinatorial properties of a mesh specified by K and its geometric shape determined by V, which is also expressed by adding V to the notation of the simplicial complex (K, V). The identification of abstract and geometric vertices is uniquely performed by the bijection Φ which relates the abstract points $\mathfrak{V}$ of K and the set of geometric points V. Any embedding of the abstract complex K into a Euclidean space induces a topology on the simplicial complex.

Definition 7 *The* underlying (topological) space $|K|$ *of a simplicial complex K immersed into $\mathbb{R}^n$ is the topological space consisting of the subset of $\mathbb{R}^n$ that is the union of all geometric realizations of simplices in K with the topology induced from any embedding of K.*

Important examples of simplicial complexes are simplicial disks and balls.

Definition 8 *A* simplicial n-ball B^n *is a simply connected simplicial complex such that $|B^n|$ is homeomorphic to the solid unit ball in $\mathbb{R}^n$, and a* simplicial n-sphere S^n *is homeomorphic to the boundary sphere of the solid unit ball in $\mathbb{R}^{n+1}$. For $n = 2$, B^2 is also called a* simplicial disk*, and S^2 is a* simplicial sphere*. For $n = 1$, S^1 is a* simplicial circle*.*

For example, an icosahedron is a simplicial sphere, and any simply closed polygon is a simplicial circle.

In some cases it makes sense to identify a simplicial complex (K, V) with its underlying set $|K|$ in a Euclidean space $\mathbb{R}^n$, for example, a polytope can always be recovered from its set of vertices. In the general case one should keep in mind that (K, V) has more the character of an immersion. For example, if the immersion of a polygonal circle intersects geometrically at a point shaping a figure-eight then it may still be a combinatorial respectively topological circle. Note that the topology of such a shape cannot be recovered solely from its shape.

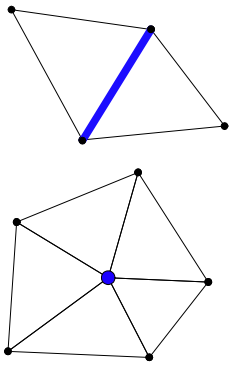

Star of an edge and a vertex.

Definition 9 *Let (K, V) be a simplicial complex. Then a subset $L \subset K$ is a* subcomplex *of K if L is a simplicial complex itself. For example, let $\sigma \in K$ be a simplex, then*

$$\operatorname{star} \sigma := \{\eta \in K \text{ that contains } \sigma, \text{ and all faces of } \eta\}$$

and

$$\operatorname{link} \sigma := \{\eta \in \operatorname{star} \sigma \mid \eta \cap \sigma = \emptyset\}.$$

are subcomplexes of K.

Simplicial surfaces extend the notion of a topological 2-manifold to the simplicial world.

Definition 10 *A* simplicial surface *S is a simplicial complex consisting of a finite set $\mathfrak{T}$ of triangles such that*

1. *Any point $p \in S$ lies in at least one triangle $T \in \mathfrak{T}$.*
2. *The star of each point $p \in S$ is a simplicial disk.*

Note, in the definition one may allow a denumerable set of triangles under the additionally assumption that the simplicial complex is locally finite, that is, the star of each vertex consists of a finite number of triangles.

A *polyhedral surface* is more general than a simplicial surface and may include flat faces with more than three vertices. The margin figure illustrates several pitfalls and degenerate situations which arise in practical implementations. The first row shows two non-manifold situations. The second row is a hanging node where adjacent faces do not join a common edge. The third row shows a valid simplicial surface consisting of four triangles where the pairwise adjacency of triangle pairs is indicated by two small lines.The right figure is a sketch to show how the middle edge belongs to all four triangles.

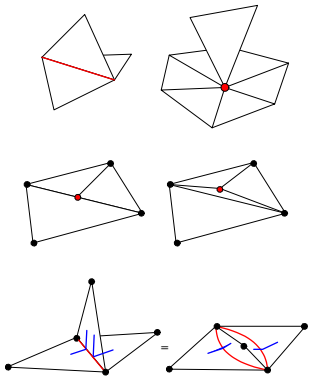

Degenerate situations and non-manifold surfaces.

Care must be taken to avoid the first two situations in practical implementations. The third situation can be resolved with an additional neighbourhood information.

Definition 11 *Let $M \subset \mathbb{R}^n$ be a topological surface. Then a simplicial surface S* triangulates *M if there exists a homeomorphism*

$$t : |S| \to M.$$

The simplicial complex S together with the homeomorphism t is called a triangulation *of M.*

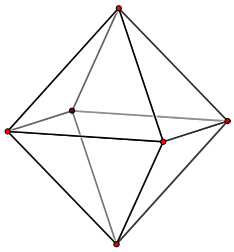

Octahedron

Smooth surfaces and simplicial surfaces are related through the following theorem, compare [20]:

Theorem 12 *The following facts hold for two-dimensional surfaces:*
(1) Any compact topological surface M in $\mathbb{R}^n$ can be triangulated, i.e. there exists a simplicial surface which triangulates M.
(2) If a topological surface is triangulated by two simplicial surfaces K_1 and K_2, then K_1 and K_2 have simplicially isomorphic subdivisions.

1.2 Distance and Metric

For metric measurements the interior of simplicial faces must be uniquely defined. Therefore, we prefer simplicial instead of polyhedral surfaces, or assure that we work with piecewise flat polygons. The metric of a surface may, for example, be induced from an immersion into a Euclidean space, or the metric may be defined in a more abstract way, say, by assigning a length to each edge which fulfills the triangle identity on each triangle. In a locally Euclidean metric the distance between two points is measured along curves whose length is measured segment-wise on the open edges and triangles:

Definition 13 *A curve γ on a simplicial complex M is called* rectifiable*, if for every simplex $\sigma \in M$ the part $\gamma_{|\sigma}$ is rectifiable w.r.t. to the smooth metric of σ. Then the* length *of γ is given by*

$$L(\gamma) := \sum_{\sigma \in M} L(\gamma_{|\mathring{\sigma}}). \tag{1.1}$$

as the sum of the lengths on each open simplex.

The area of a simplicial surface is defined in a similar way:

Definition 14 *Let M be a simplicial surface. Then we define*

$$\operatorname{area} M := \sum_{T \in M} \operatorname{area} M_{|T}. \tag{1.2}$$

Most of our considerations apply to a more general class of length spaces. Each face may have an arbitrary metric as long as the metrics of two adjacent faces are compatible, i.e. if the common edge has the same metric in both faces, and the triangle inequality holds.

In many practical applications simplicial complexes have a metric induced from an immersion into a Euclidean $\mathbb{R}^n$. For example, take a polyhedral surface in $\mathbb{R}^3$ and consider the two adjacent faces of an edge. Each face has the metric induced from $\mathbb{R}^3$, i.e. the length of any curve on a face is equal to the length of the same curve measured in $\mathbb{R}^3$. In this case, any neighbourhood of a point on the edge is isometric to a planar domain, since both faces can be unfolded to $\mathbb{R}^2$.

When considering the approximation of a smooth surface M with a sequence of polyhedral surfaces $\{M_{h,i}\}$ one should be aware that higher order terms such as area may not converge as expected. The *Schwarz lantern* is an example of a sequence of polyhedral surfaces which converges uniformly to a cylinder while the corresponding area grows to infinity.

1.3 Grids in Numerics and Graphics

In recent years an enormous effort went into the design of efficient grids in numerics and computer graphics. Adaptive grids and hierarchical representations became very important in numerical applications, and are nowadays complemented with subdivision surfaces in computer graphics modeling packages. Among the current issues is the construction of specialized encodings for efficient data compression.

This section recalls some important types of meshes used in numerical computations and computer graphics. The choice of a suitable grid depends on a number of criteria such as the shape of the domain, the type of the numerical method, or even the hardware, for example, to support parallelization of algorithms.

Structured grids tessellate a rectangle $[x_{\min}, x_{\max}] \times [y_{\min}, y_{\max}] \subset \mathbb{R}^2$ into regular quadrilaterals of the same size $h = (h_x, h_y)$. The grid Ω_h

$$\Omega_h = \left\{ (x_i, y_j) \;\middle|\; \begin{array}{ll} x_i = x_{\min} + ih_x & i \in [0, m-1] \\ y_j = y_{\min} + jh_y & j \in [0, n-1] \end{array} \right\}$$

is implicitly determined by the two extremal vertices $(x_{\min}, y_{\min})$ and $(x_{\max}, y_{\max})$ and the number of subdivisions (m, n). *Multiblock grids* use several structured grids at possibly different resolutions to cover the different regions of the domain. *Multigrids* and *sparse grids* are hierarchical representations which allow a considerable reduction of the number of grid points.

Parametric grids are obtained as images of other grid types under a continuous map Φ and thus are suitable for the discretization of more general domains. Important examples of parametric maps are Möbius maps and the Schwarz-Christoffel map, both are angle-preserving, i.e. conformal maps. Circle packings, remarkably applied by Thurston and others to problems with three-manifolds, are nowadays a promising concept in practical implementations, for example, for the flattening of rather general surfaces [14].

Unstructured or irregular grids may consist of rather general non-overlapping polygons. Such grids are determined by a set of points, i.e. the vertices of the polygons,

$$P = \{P_0, P_2, ..., P_9\}$$

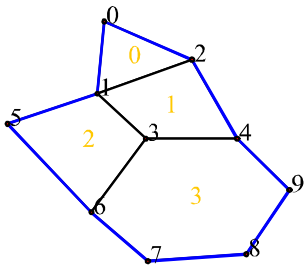

Unstructured Grid.

and connectivity information where each polygon is given as an ordered list of its vertices, or more efficient, of its vertex indices

$$\begin{aligned} E_0 &= \{0, 1, 2\} \\ E_1 &= \{2, 1, 3, 4\} \\ E_2 &= \{5, 6, 3, 1\} \\ E_3 &= \{3, 6, 7, 8, 9, 4\}. \end{aligned}$$

Additional information of a structured grid may be stored in order to achieve faster access of information, or to clarify ambiguous situations. For example, a list of neighbour faces which have common edge with the current face. The following neighbour array has for each element E_i a list of indices of adjacent elements N_i where $N_i[j]$ denotes the element adjacent to the edge $E_i[j+1]E_i[j+2]$ of E_i (indices are

modulo number of vertices of E_i).

$$\begin{aligned} N_0 &= \{1,-1,-1\} \\ N_1 &= \{2,3,-1,0\} \\ N_2 &= \{3,1,-1,-1\} \\ N_3 &= \{-1,-1,-1,-1,1,2\}. \end{aligned}$$

The naming convention has its origin in triangle meshes where the edge $E_i[j+1]E_i[j+2]$ is opposite to the vertex E_i. The above rule allows us to use the same programming code for both, simplicial as well as polyhedral surfaces.

An alternative to vertex based formats are *facet-edges formats*. Here a set of edges is given as above by specifying pairs of vertex indices. Then higher dimensional cells are defined through their boundary, that means a two-dimensional element is determined by a set of edge indices. Such formats are useful if all cells of a cell-complex play an active role and have associated information.

A wealth of meshes is used in computer graphics and numerics for different purposes. *Progressive meshes* introduced by Hoppe [12] are based on vertex-split and edge-collapse operations for adaptive refinement and coarsening. In recent years these data types have been very popular in computer graphics especially since they allow topology changes. They are a special class of *multi-resolution grids* or *hierarchical grids* which store different levels of resolution of a shape. Often a smooth transition between different hierarchical resolutions is incorporated in the data structure. *Normal meshes* [11] were designed to describe shapes locally as graph over a coarser resolution of the same mesh. This technique is especially suitable for *subdivision surfaces* or multi-resolution surfaces obtained from a wavelet decomposition where the finer resolutions are obtained algorithmically.

The fast and incremental transmission of shapes over low-bandwidth connections plays an increasing role nowadays. Here specialized representations of meshes allow a compressed encoding. For example, the algorithm by Taubin and Rossignac [36], which is incorporated into the MPEG-4 standard, encodes the connectivity of a triangle mesh with about $2-3$ bits per vertex compared to 96 bits used in the index based representation mentioned above.

1.4 Finite Element Spaces

Piecewise polynomial functions on simplicial surfaces conceptually fall into the category of finite element spaces. Here we briefly recall the most basic function spaces relevant for our later work. See the books [5][4] for an introduction.

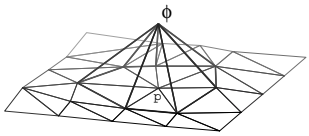

Basis function on manifold.

Definition 15 *On a simplicial surface M_h we define the function space S_h of* conforming finite elements*:*

$$S_h := \left\{ v : M_h \to \mathbb{R}^d \;\middle|\; v \in C^0(M_h) \text{ and } v \text{ is linear on each triangle} \right\}$$

S_h is a finite dimensional space spanned by the Lagrange basis functions $\{\varphi_1, .., \varphi_n\}$ corresponding to the set of vertices $\{p_1, ..., p_n\}$ of M_h, that is for each vertex p_i we have a function

$$\begin{gathered} \varphi_i : M_h \to \mathbb{R},\ \varphi_i \in S_h \\ \varphi_i(p_j) = \delta_{ij} \quad \forall i, j \in \{1, .., n\} \\ \varphi_i \text{ is linear on each triangle.} \end{gathered} \tag{1.3}$$

Then each function $u_h \in S_h$ has a unique representation

$$u_h(p) = \sum_{j=1}^{n} u_j \varphi_j(p) \quad \forall\, p \in M_h$$

where $u_j = u_h(p_j) \in \mathbb{R}^d$. The function u_h is uniquely determined by its nodal vector $(u_1, ..., u_n) \in \mathbb{R}^{dn}$.
Sometimes we will also use piecewise higher-order polynomial representations described in a similar way with different basis functions. Note that any component function of a function $v \in S_h$ has bounded Sobolev H^1 norm.

1.4.1 Non-Conforming Finite Elements

In our later investigations the following space of non-conforming finite elements, see [5][4] for a detailed discussion, plays an important role. Since these spaces include discontinuous functions their use is often titled as a *variational crime* in the finite element literature. In our settings, non-conforming functions naturally appear as the correct spaces for our later considerations on constant mean curvature surfaces.

Definition 16 *For a simplicial surface M_h, we define the space of* non-conforming finite elements *by*

$$S_h^* := \left\{ v : M_h \to \mathbb{R}^d \;\middle|\; \begin{array}{l} v_{|T} \text{ is linear for each } T \in M_h, \text{ and} \\ v \text{ is continuous at all edge midpoints} \end{array} \right\}$$

The space S_h^* is no longer a finite dimensional subspace of $H^1(M_h)$ as in the case of conforming elements, but S_h^* is a superset of S_h. Let $\{m_i\}$ denote the set of edge midpoints of M_h, then for each edge midpoint m_i we have a basis function

$$\begin{array}{c} \psi_i : M_h \to \mathbb{R} \quad \psi_i \in S_h^* \\ \psi_i(m_j) = \delta_{ij} \quad \forall\, i,j \in \{1,2,..\} \\ \psi_i \text{ is linear on each triangle.} \end{array} \tag{1.4}$$

The support of a function ψ_i consists of the (at most two) triangles adjacent to the edge e_i, and ψ_i is usually not continuous on M_h. Each function $v \in S_h^*$ has a representation

$$v_h(p) = \sum_{\text{edges } e_i} v_i \psi_i(p) \quad \forall\, p \in M_h$$

where $v_i = v_h(m_i)$ is the value of v_h at the edge midpoint m_i of e_i. Let $M_h \subset \mathbb{R}^m$ be a conforming triangulation with vertices $V = \{p_1, p_2, ...\}$ and edge midpoints $E = \{m_1, m_2, ...\}$. For a given triangle $t \in M_h$ with vertices $\{p_{t_1}, p_{t_2}, p_{t_3}\}$ and edge midpoints $\{m_{t_1}, m_{t_2}, m_{t_3}\}$ we have the following elementary correspondence

$$\frac{1}{2} \begin{pmatrix} 0 & 1 & 1 \\ 1 & 0 & 1 \\ 1 & 1 & 0 \end{pmatrix} \begin{pmatrix} p_{t_1} \\ p_{t_2} \\ p_{t_3} \end{pmatrix} = \begin{pmatrix} m_{t_1} \\ m_{t_2} \\ m_{t_3} \end{pmatrix} \tag{1.5}$$

respectively

$$\begin{pmatrix} -1 & 1 & 1 \\ 1 & -1 & 1 \\ 1 & 1 & -1 \end{pmatrix} \begin{pmatrix} m_{t_1} \\ m_{t_2} \\ m_{t_3} \end{pmatrix} = \begin{pmatrix} p_{t_1} \\ p_{t_2} \\ p_{t_3} \end{pmatrix}. \tag{1.6}$$

We will also use the term *non-conforming surface* to denote a simplicial surface where adjacent triangles are connected at the midpoint of their common edge but may be twisted. Later we also require that the corresponding edge of two adjacent triangles must have the same length. Non-conforming surfaces may be considered as images of a non-conforming map from a conforming surface, therefore, we often do not distinguish between a non-conforming surface and a non-conforming map.

2

Conjugation of Discrete Harmonic Maps

Discrete harmonic maps appear as a basic model problem in finite element theory and differential geometry for the discretization of smooth concepts. Beyond that, discrete harmonic maps have a wide range of non-trivial applications in computer graphics, for example to smoothen noisy meshes, or in differential geometry to compute constant mean curvature surfaces.

Several discrete operators on simplicial surfaces are related to discrete harmonic maps. For example, the area gradient, the mean curvature, or the divergence operator on vector fields. The main topic of this section is the construction of pairs of conjugate discrete Laplace-Beltrami harmonic maps on polyhedral surfaces. We start to derive the definitions and properties of discrete harmonic maps in a geometric setting which will then allow us to develop other discrete geometric operators and to solve problems related to minimal and constant mean curvature surfaces in Section 3.

Harmonic maps on surfaces also have practical importance, for example, we derive in Section 3 efficient numerical algorithms for solving free boundary value problems for unstable minimal surfaces and constant mean curvature surfaces. In the algorithms [25] and [23], the conjugate of a minimal surface is obtained via the conjugation of a discrete harmonic map. Conjugate harmonic maps are originally defined on the dual graph of the edge graph of the original surface but

one should consider them as non-conforming functions. The results of the present chapter provide a thorough understanding of the geometric constructions used in Pinkall and Polthier [25] and in Oberknapp and Polthier [23] by relating the discrete conjugation of surfaces to non-conforming finite element spaces.

Convergence of conforming harmonic maps has been shown by Tsuchiya [37]. As a more general result for surfaces, Dziuk and Hutchinson [8] obtained optimal convergence results in the H^1 norm for the finite element procedure of the Dirichlet problem of surfaces with prescribed mean curvature. Compare Müller et al. [21] for harmonic maps on planar lattices using the five-point Laplacian.

In a subsequent section we will apply the duality between discrete harmonic maps and their conjugates to define discrete conformal maps. We will extend a conformal energy proposed by Hutchinson [15] to the discrete spaces $S_h \times S_h^*$ and show that the discrete holomorphic maps have zero conformal energy, a property generically not available for conforming piecewise linear maps.

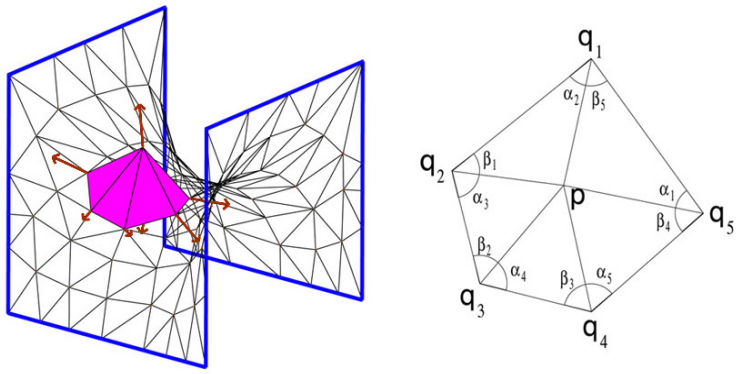

FIGURE 2.1. Discrete mean curvature vector on a polyhedral surface given as Laplace-Beltrami operator of the identity map from the surface to itself.

We start with a review of the Dirichlet problem of harmonic maps in Section 2.1 followed by the discretization using conforming Lagrange elements in Section 2.2. In Section 2.3 we discretize the same Dirichlet problem using the non-conforming Crouzeix-Raviart elements, and derive a pointwise expression of the discrete minimality condition. Section 2.4 contains the main results of this chapter, namely, identifying solutions in both finite element spaces as pairs of discrete conjugate harmonic maps. Applications of the results are given in

Section 3 to the conjugation of discrete minimal and constant mean curvature surfaces.

2.1 Review of Smooth Harmonic Maps

On a Euclidean domain, the Laplace operator is given by the second partial derivatives

$$\Delta = \frac{\partial}{\partial x_1^2} + ... + \frac{\partial}{\partial x_n^2}.$$

Harmonic maps $u : \Omega \to \mathbb{R}$ on an open set Ω in $\mathbb{R}^n$ are solutions of the Laplace equation

$$\Delta u = 0 \text{ in } \Omega \tag{2.1}$$

which often appears with prescribed boundary conditions. Dirichlet conditions prescribe fixed boundary values in the form of a function g

$$u_{|\partial\Omega} = g \text{ on } \partial\Omega$$

and Neumann conditions prescribe the derivative of u in the direction of the normal ν of the boundary

$$\partial_\nu u_{|\partial\Omega} = \mu \text{ on } \partial\Omega.$$

Dirichlet and Neumann boundary conditions may appear simultaneously on disjoint segments of the boundary.

The Laplace operator of vector-valued maps, and thereby the harmonicity of vector-valued maps, is defined component-wise on each coordinate function. For functions $u : M \to \mathbb{R}$ on a manifold M with a Riemannian metric g the Laplace-Beltrami operator Δ_g is a generalization of the Laplace operator. Assume normal coordinates around a point p on M and let $\{e_1, ..., e_n\}$ be the induced orthonormal frame in the tangent space of M, then

$$\Delta_g = \nabla_{e_1}\nabla_{e_1} + ... + \nabla_{e_n}\nabla_{e_n}.$$

Harmonic maps also appear as minimizers of the *Dirichlet energy*

$$E_D(u) = \frac{1}{2}\int_M |\nabla u|^2 \, dx \tag{2.2}$$

with Dirichlet conditions (or Neumann) at the boundary, since the Laplace equation 2.1 is the Euler-Lagrange equation of the Dirichlet energy. To see this, let $u(t) := u_0 + t\phi : M \to \mathbb{R}$ be any C^1-variation of

a function u_0 whose variation function has compact support $\phi_{|\partial M} = 0$. Then by differentiation and integration by parts we obtain

$$\begin{aligned} \frac{d}{dt}_{|t=0} E_D(u(t)) &= \int_M < \nabla u, \nabla \phi > \\ &= -\int_M \Delta u \cdot \phi + \int_{\partial M} \partial_v u \cdot \phi \end{aligned}$$

where v is the exterior normal along ∂M. Since ϕ has compact support, the last integrand vanishes identically. Since the above equation holds for any C^1-variation we derive

$$\nabla E_D(u) = 0 \Longleftrightarrow \Delta u = 0$$

from the fundamental lemma of the calculus of variations. The minimizer $u_{\min}$ is unique since

$$\begin{aligned} E_D(u_{\min} + \phi) &= E_D(u_{\min}) + E_D(\phi) \\ &> E_D(u_{\min}) \quad \forall\ \phi_{|\partial M} = 0, \phi \neq 0. \end{aligned}$$

where the cross term vanishes because of the minimality condition for $u_{\min}$.

2.2 Discrete Dirichlet Energy

There are different equivalent ways to introduce discrete harmonic maps. Here we use the characterization of harmonic maps as minimizers of the Dirichlet energy since this approach also provides an efficient numerical algorithm to solve the boundary value problems for discrete harmonic maps.

Definition 17 *Let M_h be a simplicial surface in $\mathbb{R}^m$ and S_h the set of polyhedral maps on M_h. Then the* Dirichlet energy *of a function $u_h \in S_h$ with $u_h : M_h \to \mathbb{R}^d$ is given by*

$$E_D(u_h) := \frac{1}{2} \sum_{T \in \mathfrak{T}_h} \int_T |\nabla u_h|^2 \, dx. \tag{2.3}$$

That is, the Dirichlet energy of u_h is the sum of the Dirichlet energies of the smooth atomic maps $u_{h|T}$ on each triangle T.

Now we consider critical points of the Dirichlet energy. For simplicity, we restrict to interior variations which keep the boundary values fixed.

Definition 18 *A* variation $\phi(t) \in S_h$, $t \in [0, \varepsilon)$, *is a family of functions differentiable in* t *such that each map* $u_h \in S_h$ *gives rise to a family of maps* $u_h(t) \in S_h$ *with*

$$u_h(t) = u_h + \phi(t)$$

Basically, a variation of a function $u_h \in S_h$ is a modification of its values at each vertex p_i of the triangulation M_h given by $u_h(t)(p_i) = u_h(p_i) + \phi(t)(p_i)$. For simplicity, we restrict to Dirichlet boundary conditions, that is, the variations $\phi(t)$ are zero along the boundary of M_h.

Definition 19 *A critical point* u_h *in* S_h *of the Dirichlet energy (2.3) in* S_h *with respect to Dirichlet boundary conditions is called a* discrete harmonic map.

In the following we derive an explicit representation of the Dirichlet energy of polyhedral maps and a system of equations for the discrete minimizers which characterize discrete harmonic maps.

Let $T = \{p_1, p_2, p_3\}$ be a triangle of a simplicial surface and oriented edges $\{c_1, c_2, c_3\}$ with $c_i = p_{i-1} - p_{i+1}$, and $\varphi_i : T \to \mathbb{R}$ be the Lagrange basis function at vertex p_i with $\varphi_i(p_j) = \delta_{ij}$. Then its gradient is

$$\nabla\varphi_{i|T} = \frac{1}{2\,\mathrm{area}\,T} J c_i, \tag{2.4}$$

where J denotes rotation by $\frac{\pi}{2}$ oriented such that Jc_i points into the triangle. Note, that $\varphi_1+\varphi_2+\varphi_3 = 0$ implies $\nabla\varphi_i = -\nabla\varphi_{i-1} - \nabla\varphi_{i+1}$. The basis functions have mutual scalar products given by

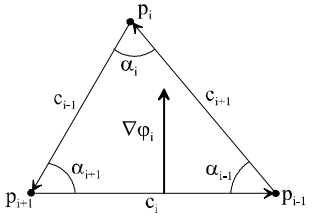

Gradient of basis function.

$$\begin{aligned} \langle \nabla\varphi_{i-1}, \nabla\varphi_{i+1} \rangle &= -\frac{\cot\alpha_i}{2\,\mathrm{area}\,T} \\ \langle J\nabla\varphi_i, \nabla\varphi_{i+1} \rangle &= \frac{1}{2\,\mathrm{area}\,T} \\ |\nabla\varphi_i|^2 &= \frac{\cot\alpha_{i-1} + \cot\alpha_{i+1}}{2\,\mathrm{area}\,T}. \end{aligned} \tag{2.5}$$

Since each function $u_h \in S_h$ has a representation

$$u_h(p) = \sum_{j=1}^{n} u_j \varphi_j(p) \quad p \in M_h,$$

where $u_j = u_h(p_j)$ denotes the function value of u_h at the vertex p_j of M_h, on a single triangle T the gradient of $u_{h|T} : T \longrightarrow \mathbb{R}^d$ is given by

$$\nabla u_{h|T} = \frac{1}{2\,\mathrm{area}\,T} \sum_{j=1}^{3} u_j J c_j. \tag{2.6}$$

Theorem 20 *Let M_h be a simplicial surface and S_h the set of continuous and piecewise linear functions on M_h. Then the discrete Dirichlet energy of any function $u_h \in S_h$ is given by*

$$E_D(u_h) = \frac{1}{4} \sum_{edges\ (x_i,x_j)} (\cot \alpha_{ij} + \cot \beta_{ij}) \left| u_h(p_i) - u_h(p_j) \right|^2 . \quad (2.7)$$

Further, the minimizer of the Dirichlet functional (2.3) is unique and solves

$$\frac{d}{du_i} E_D(u_h) = \frac{1}{2} \sum_{x_j \in n(x_i)} (\cot \alpha_{ij} + \cot \beta_{ij})(u_h(p_i) - u_h(p_j)) = 0 \quad (2.8)$$

at each interior vertex p_i of M_h. The first summation runs over all edges of the triangulation, and the second summation over all edges emanating from p_i. The angles α_{ij} and β_{ij} are vertex angles lying opposite to the edge (p_i, p_j) in the two triangles adjacent to (p_i, p_j).

Proof. Using the explicit representation (2.4) of the basis functions and the identity $\nabla\varphi_i = -\nabla\varphi_{i-1} - \nabla\varphi_{i+1}$, we obtain the Dirichlet energy of $u_{h|T}$:

$$\begin{aligned} E_D(u_{h|T}) &= \frac{1}{2} \int_T - \sum_{j=1}^{3} |u_{j+1} - u_{j-1}|^2 \left\langle \nabla\varphi_{j-1}, \nabla\varphi_{j+1} \right\rangle \\ &= \frac{1}{4} \sum_{j=1}^{3} \cot \alpha_j \left| u_{j+1} - u_{j-1} \right|^2 . \end{aligned}$$

Summation over all triangles of M_h and combining the two terms corresponding to the same edge leads to equation 2.7.

At each interior vertex p_i of M_h, the gradient of E_D with respect to variations of $u_i = u_h(p_i)$ in the image of u_h is obtained by partial differentiation and easily derived from

$$\frac{d}{du_i} E_D(u_h) = \int_\Omega \left\langle \nabla u_h, \nabla\varphi_i \right\rangle .$$

Since S_h is a finite dimensional space, the quadratic minimization problem for the Dirichlet energy has a unique solution u_h in S_h. □

The definition of the Dirichlet energy of vector-valued maps $F_h : M_h \to N_h \subset \mathbb{R}^d$ is in full coherence with the definition of Dirichlet energy of scalar-valued maps. Namely, if the map $F_h = (f_1, .., f_d)$ has component functions $f_i : M_h \to \mathbb{R}$ then we have

$$E_D(F_h) = \sum_{i=1}^{d} E_D(f_i)$$

since $|\nabla F_h|^2 = |\nabla f_1|^2 + .. + |\nabla f_d|^2$. Vector-valued harmonic maps are defined as critical values of the Dirichlet functional in the same way as in the scalar-valued case. Therefore, the balancing condition for scalar-valued harmonic maps directly gives a balancing formula for vector-valued discrete harmonic maps too.

The following definition includes more general boundary conditions. Neumann boundary conditions constrain the derivative of a function in direction of the exterior normal of the domain. Later we will make use of other boundary conditions which are useful for maps from a simplicial surface M_h to another surface N_h.

Definition 21 *A solution $u_h \in S_h$ of the Dirichlet problem (2.8) in S_h is called a* discrete harmonic map. *To include symmetry properties into this definition we allow in some cases also variation of boundary points:*

- *if a domain boundary arc and its corresponding image boundary arc are straight lines, then the interior boundary points may vary along the straight line in image space*
- *if both corresponding arcs are planar symmetry curves restricted to planes we allow variation of interior boundary points in the image plane. This models also free boundary value problems*
- *in all other cases the image boundary points remain fixed.*

Remark 22 *At each vertex x_i Equation (2.8) can be geometrically interpreted as a balancing condition for the weighted edges emanating from the vertex x_i. The weight of each edge solely depends on the angles in the base surface M_h, i.e. the weights depend only on the conformal structure of M_h.*

Examples of Discrete Harmonic Maps

Simple examples of discrete harmonic maps are derived from the observation that on the integer grid $\mathbb{Z} \times \mathbb{Z}$ in $\mathbb{R}^2$ the interpolants of some smooth harmonic functions are discrete harmonic:

Example 23 *On a rectangular $\mathbb{Z} \times \mathbb{Z}$ grid in $\mathbb{R}^2$, which is triangulated by subdividing along either diagonal of each rectangle, the interpolating functions of*

$$\operatorname{Re} z, \operatorname{Re} z^2, \operatorname{Re} z^3, \text{ and } \operatorname{Im} z^4$$

are discrete harmonic maps, and so are the interpolants of some other polynomials.

Example 24 *On a rectangular $\mathbb{Z} \times \mathbb{Z}$ grid in $\mathbb{R}^2$, the weight of each diagonal is $\cot \frac{\pi}{2}$, and it vanishes independent of the chosen diagonal in each square. Therefore, at each grid point (i, j) only the discrete values of the* five-point stencil

$$\{(i,j),(i,j-1),(i-1,j),(i+1,j),(i,j+1)\} \quad i,j \in \mathbb{Z}$$

of the finite difference Laplacian contribute to the Dirichlet gradient.

The next example leads to discrete harmonic maps on a simplicial surfaces using linear maps:

Definition 25 *Let M_h be a polyhedral surface in $\mathbb{R}^m$. A map $u_h \in S_h(M_h)$ from M_h to $\mathbb{R}^d$ is called a* linear map *if u_h is the restriction $u_{|M}$ of a linear map $u : \mathbb{R}^m \to \mathbb{R}^d$, i.e.*

$$u_h = u_{|M} : M_h \to \mathbb{R}^d.$$

For example, any coordinate function $x_i : M_h \to \mathbb{R}$ on a polyhedral surface M_h is a linear map, and, more general, let $a \in \mathbb{R}^m$ be a constant vector, then

$$u_h(p) := \langle a, p \rangle \quad \forall\, p \in M_h$$

is linear.
On an arbitrary simplicial surface $M_h \subset \mathbb{R}^m$ the following geometric assumption on the underlying domain surface M_h leads to discrete harmonic functions:

Example 26 *All linear maps $u_h : M_h \to \mathbb{R}^d$ on a polyhedral surface M_h are discrete harmonic if and only if M_h is a discrete minimal surface.*

Proof. Using the Lagrange basis functions $\varphi_i : M_h \to \mathbb{R}$ associated to each vertex p_i of M_h we have the representation

$$u_h(x) = \sum_{p_i \in M_h} u_h(p_i)\varphi_i(p), \quad p \in M_h.$$

The gradient of the Dirichlet energy can be transformed using the linearity of u_h

$$\begin{aligned}\frac{d}{du_i}E_D(u_h) &= \frac{1}{2}\sum_{j\in n(i)}\left(\cot\alpha_{ij}+\cot\beta_{ij}\right)\left(u_h(p_i)-u_h(p_j)\right)\\ &= u_h(\frac{1}{2}\sum_{j\in n(i)}\left(\cot\alpha_{ij}+\cot\beta_{ij}\right)\left(p_i-p_j\right))\\ &= u_h(\frac{d}{dp_i}E_D(\mathrm{id}_h\, M_h)).\end{aligned}$$

Therefore, u_h is a critical value of the Dirichlet energy if and only if the identity map of M_h is discrete harmonic. The harmonicity of the identity map of a discrete minimal surface is shown in Corollary 48. □

Mean Value Property and Maximum Principle

Among the two most important properties of smooth harmonic maps are the mean value property and the maximum principle.
Mean Value Property: Let $p \in M$ and $U_\varepsilon(p)$ be a disk with radius ε around p. Then the value of a smooth harmonic function u at the center p is the average of the values along the boundary of the disk

$$u(p) = \frac{1}{2\pi\varepsilon}\int_{|q-p|=\varepsilon} u(q).$$

We obtain a discrete version for polyhedral maps if we replace the disk with a regular polygon.

Lemma 27 *Let u_h be a discrete harmonic map defined on a simplicial surface M_h. If the* star *of a vertex p consists of congruent isosceles triangles centered at p then*

$$u_h(p) = \frac{1}{\#\operatorname{link} p}\sum_{q_j\in\operatorname{link} p} u_h(q_j)$$

is the center of mass of the function values $\{u_h(q_j)\}$ on the link of p.

Proof. All vertex angles appearing in Equation (2.8) are the same. □

Maximum Principle: Since smooth harmonic maps solve an elliptic differential equation they satisfy a maximum principle. This means, in any open domain $U \subset M$ the maximum and minimum of u is attained

at the boundary ∂U. In the discrete case, a similar statement for the star of a vertex does not hold in general, for example, it may fail if the spatial domain contains angles larger than 90 degrees.

Lemma 28 *Let u_h be a discrete harmonic map defined on a spatial domain of a simplicial surface M_h formed by the points $\{q_j\}$ around a vertex p. If the triangles around p are all acute, then $u_h(p)$ is contained in the convex hull of the points $\{u_h(q_j)\}$.*

Proof. From the local harmonicity condition (2.8) we see that $u_h(p)$ can be represented as a linear combination of the points $\{u_h(q_j\}$. Since all relevant angles are acute the weights of the $u_h(q_j)$ are in the interval $(0, 1)$, and $u_h(p)$ is a convex combination. □

The two previous lemmas do not hold if we allow more general domains. For example, if the domain contains obtuse triangles as in the Example 3.4 then neither the mean value nor the convex hull property may be valid.

The non-convexity of discrete harmonic maps will lead to interesting counterexamples of the maximum principle of minimal surfaces in Section 3. In practical applications, for example, when smoothing meshes with a Laplace filtering or mapping surfaces onto a planar domain, then one would often like to ensure convexity. In these case the mesh parametrization by Floater [9] might be a useful strategy since it ensures convexity.

2.3 Non-Conforming Harmonic Maps

Non-conforming maps on simplicial surfaces were introduced in Section 1.4.1 as another natural set of discrete maps. Let M_h be a simplicial surface then we state the Dirichlet energy in the space S_h^* as in the previous section.

Definition 29 *Let M_h be a simplicial surface in $\mathbb{R}^m$. Then the* Dirichlet energy *of a function $v_h \in S_h^*$ with $v_h : M_h \to \mathbb{R}^d$ is given by*

$$E_D(v_h) := \frac{1}{2} \sum_{T \in M_h} \int_T |\nabla v_h|^2 \, dx.$$

That is, the Dirichlet energy of v_h is the sum of the Dirichlet energies of the smooth atomic maps $v_{h|T}$ on each triangle T.

Now we consider critical points of the Dirichlet energy, and again, for simplicity, we restrict to interior variations which keep the boundary values fixed.

Definition 30 *A* variation $\Psi(t) \in S_h^*$, $t \in [0, \varepsilon)$, *is a family of functions differentiable in* t *such that each map* $v_h \in S_h^*$ *rise to a family of maps* $v_h(t) \in S_h^*$ *with*

$$v_h(t) = v_h + \Psi(t)$$

Basically, a variation of a function $v_h \in S_h^*$ is a modification of its values at each edge midpoint m_i of the simplicial surface M_h given by $v_h(t)(m_i) = v_h(m_i) + \Psi(t)(m_i)$. For simplicity, we restrict to Dirichlet boundary conditions, that is, the variations $\Psi(t)$ are zero at midpoints of boundary edges of M_h.

Definition 31 *A critical point* v_h *in* S_h^* *of the Dirichlet energy (2.3) in* S_h^* *with respect to Dirichlet boundary conditions is called a* (non-conforming) discrete harmonic map.

Using the identities in an Euclidean triangle T with vertices $\{p_1, p_2, p_3\}$ and oriented edges $\{c_1, c_2, c_3\}$ with $c_i = p_{i-1} - p_{i+1}$, we obtain on T the following representation of the basis functions $\psi_i \in S_h^*$ corresponding to edge c_i :

$$\nabla \psi_i = -2 \nabla \varphi_i = \frac{-1}{\operatorname{area} T} J c_i, \tag{2.9}$$

where $\varphi_i \in S_h$ is the conforming basis function corresponding to the triangle vertex p_i opposite to the edge c_i, and J is the rotation of an edge by $\frac{\pi}{2}$ such that Jc points in the opposite direction of the outer normal of the triangle.

Theorem 32 *Let* $v \in S_h^*$ *be a non-conforming function on a simplicial surface* M_h. *Then the Dirichlet energy of* v_h *has the explicit representation*

$$E_D(v) = \sum_{all\ edges\ c_i} \cot \alpha_i \left| v_{i_{-2}} - v_{i_{-1}} \right|^2 + \cot \beta_i \left| v_{i_1} - v_{i_2} \right|^2. \tag{2.10}$$

where $\{i_{-2}, i_{-1}, i_1, i_2, \}$ *denote indices of adjacent edge midpoints as shown in Figure 2.2, and* v_{i_j} *denotes the value* $v(m_{i_j})$. *The angles are measured on* M_h.

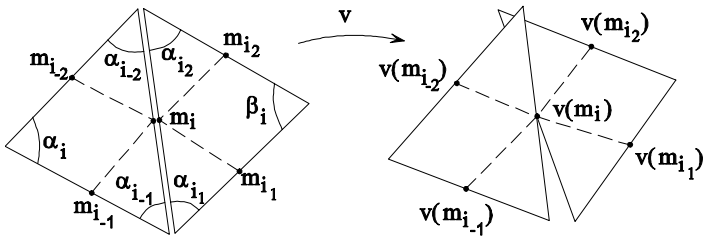

FIGURE 2.2. A non-conforming map is given by its values on edge midpoints.

The unique minimizer of the Dirichlet functional on M_h solves a system of equations such that at each edge midpoint m_i we have

$$\begin{aligned}\frac{d}{dv_i}E_D(v) &= 2(\cot\alpha_{i_{-2}}(v_i - v_{i_{-1}}) + \cot\alpha_{i_{-1}}(v_i - v_{i_{-2}}) \\ &\quad + \cot\alpha_{i_1}(v_i - v_{i_2}) + \cot\alpha_{i_2}(v_i - v_{i_1})) \\ &= 0.\end{aligned} \tag{2.11}$$

Proof. Since $\nabla\psi_i = -2\nabla\varphi_i$, the representation of the Dirichlet energy is a consequence of the explicit representation for conforming elements (2.7). On a single triangle T,

$$\begin{aligned}E_D(v_{|T}) &= \frac{1}{2}\int_T -\sum_{j=1}^{3}|v_{j+1} - v_{j-1}|^2\left\langle\nabla\psi_{j-1}, \nabla\psi_{j+1}\right\rangle \\ &= \sum_{j=1}^{3}\cot\alpha_j\,|v_{j+1} - v_{j-1}|^2\,.\end{aligned}$$

The support of a component of the gradient of the Dirichlet energy consists of those two triangles adjacent to the edge corresponding to this variable. Equation (2.11) follows directly from the representation on a single triangle T with edges $\{c_1, c_2, c_3\}$ and $c_1 + c_2 + c_3 = 0$

$$\begin{aligned}\frac{d}{dv_i}E_D(v_{|T}) &= \int_T\left\langle\nabla v_{|T}, \nabla\psi_i\right\rangle = \frac{1}{\operatorname{area}T}\sum_{j=1}^{3}v_j\left\langle c_j, c_i\right\rangle \\ &= 2\cot\alpha_{i-1}(v_i - v_{i+1}) + 2\cot\alpha_{i+1}(v_i - v_{i-1})\end{aligned}$$

by combining the expression for the two triangles in the support of ψ_i. □

2.4 Conjugate Harmonic Maps

Discrete harmonic maps have been well studied as a basic model problem in finite element theory, while the definition of the conjugate of a discrete harmonic map was not completely settled. In this section we are interested in pairs of discrete harmonic maps on a Riemann surface M which are both minimizers of the Dirichlet energy

$$E(u) = \frac{1}{2}\int_M |\nabla u|^2 \, dx,$$

and are conjugate, i.e. solutions of the Cauchy Riemann equations

$$dv = *du.$$

We note that generically such pairs do not exist in the space of piecewise linear conforming Lagrange finite elements S_h but the problem naturally leads to the space of piecewise linear non-conforming Crouzeix-Raviart elements S_h^*. S_h alone is too rigid to contain the conjugate of a generic discrete harmonic function.

We define the conjugate harmonic maps of discrete harmonic maps in S_h and in S_h^*. A smooth harmonic map $u : M \to \mathbb{R}$ on an oriented Riemannian surface M and its conjugate harmonic map $u^* : M \to \mathbb{R}$ solve the Cauchy-Riemann equations

$$du^* = *du$$

where $*$ is the Hodge star operator with respect to the metric in M. In the discrete version, we denote by J the rotation through $\frac{\pi}{2}$ in the oriented tangent space of M, and start with a locally equivalent definition as Ansatz:

Definition 33 *Let $u \in S_h$, respectively S_h^*, be a discrete harmonic map on a simplicial surface M_h with respect to the Dirichlet energies in S_h, respectively S_h^*. Then its conjugate harmonic map u^* is defined by the requirement that it locally fulfills*

$$\nabla u^*_{|T} = J\nabla u_{|T} \quad \forall \text{ triangles } T \in M_h. \tag{2.12}$$

The remainder of the section is devoted to prove that the discrete conjugate map is well-defined by showing the closedness of the differential $*du$, and to prove the harmonicity properties of its integral u^*.

To avoid case distinctions we represent each function with respect to the basis functions ψ_i of S_h^* such that on each triangle

$$u_{|T} = \sum_{i=1}^{3} u_i \psi_i,$$

where u_i is the function value of u at the midpoint of edge c_i. We use the same notation for $u^*_{|T}$, and obtain by Definition 2.12

$$\sum_{i=1}^{3} u_i^* \nabla \psi_i = \sum_{i=1}^{3} u_i J \nabla \psi_i. \tag{2.13}$$

Lemma 34 *Let T be a triangle with oriented edges $\{c_1, c_2, c_3\}$, $c_1 + c_2 + c_3 = 0$. A pair of linear functions u and u^* related by Equation (2.13), has values at edge midpoints related by*

$$\begin{pmatrix} u_3^* - u_1^* \\ u_3^* - u_2^* \end{pmatrix} = \begin{pmatrix} \cot\alpha_3(u_2 - u_1) + \cot\alpha_1(u_2 - u_3) \\ \cot\alpha_3(u_2 - u_1) + \cot\alpha_2(u_3 - u_1) \end{pmatrix} \tag{2.14}$$

Proof. The representation (2.9) of $\nabla\psi_i$ converts Equation (2.13) to

$$\sum_{i=1}^{3} u_i^* J c_i = \sum_{i=1}^{3} u_i c_i.$$

Using $-c_3 = c_1 + c_2$, we express the left side of the above equation as a vector in the span of $\{Jc_1, Jc_2\}$

$$(u_3^* - u_1^*)\, Jc_1 + (u_3^* - u_2^*)\, Jc_2 = \sum_{i=1}^{3} u_i c_i.$$

If the triangle T is nondegenerate, then the matrix (Jc_1, Jc_2) has rank 2, and scalar multiplication with c_1 and c_2 yields

$$\begin{pmatrix} u_3^* - u_1^* \\ u_3^* - u_2^* \end{pmatrix} = \frac{2}{\operatorname{area}(T)} \sum_{i=1}^{3} u_i \begin{pmatrix} \langle c_2, c_i \rangle \\ -\langle c_1, c_i \rangle \end{pmatrix},$$

which easily transforms to Equation (2.14). □

Now we consider a discrete harmonic map $u \in S_h$ and prove local exactness of its discrete conjugate differential.

Proposition 35 *Let M_h be a simply connected simplicial surface and $u \in S_h$ with $u : M_h \longrightarrow \mathbb{R}^d$ an edge continuous discrete harmonic function. Then the discrete Cauchy-Riemann equations (2.12) have a globally defined solution $u^* : M_h \longrightarrow \mathbb{R}^d$ with $u^* \in S_h^*$. Two solutions u_1^* and u_2^* differ by an additive integration constant.*

Proof. We define the discrete differential du^* of u^* such that on each triangle T

$$du^*_{|T} := *du_{|T}.$$

Since $u_{|T}$ is a linear map, the conjugate differential $du^*_{|T}$ is well defined and there exists a unique smooth solution $u^*_{|T}$ of the smooth Cauchy-Riemann equations on T, up to an additive constant. By Lemma 34, $u^*_{|T}$ is explicitly given in terms of $u_{|T}$ and T.
If $u \in S_h$ is a discrete harmonic map then it turns out that du^* is closed along closed paths on M_h that cross edges only at their midpoints. Since du^* is closed inside each triangle, it is sufficient to prove closedness for a path γ in the vertex star of a vertex $p \in M_h$ such that $\gamma_{|T}$ linearly connects the midpoints of the two edges of T having p in common, see Figure 2.3. Let $\{m_1, .., m_k\}$ be the sequence

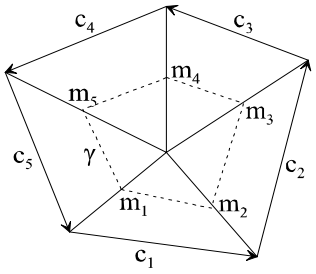

FIGURE 2.3. Dual edge graph γ around a vertex.

of edge midpoints determining γ. The edges $d_j := m_{j+1} - m_j$ of γ are parallel to c_j with $c_j = 2d_j$. We use Equation (2.14) in each triangle to derive

$$\begin{aligned}\int_\gamma du^* &= \sum_{j=1}^{k} \int_{\gamma_{|T_j}} *du_{|T_j} = \sum_{j=1}^{k} < J\nabla u_{|T_j}, d_j > \\ &= -\frac{1}{2} \sum_{j=1}^{k} < \nabla u_{|T_j}, Jc_j >= 0,\end{aligned}$$

since u is harmonic in S_h, see Equation (2.8). Therefore, du^* is closed along the dual edge graph through the edge midpoints of M_h, and $u^* \in S^*_h$ is globally defined on simply connected regions of M_h. □
For a harmonic map $u \in S_h$, the following proposition proves harmonicity of the conjugate map $u^* \in S^*_h$.

Proposition 36 *Let $u \in S_h$ be a discrete harmonic map on a simplicial surface M_h and let $u^* \in S_h^*$ be a solution of the discrete Cauchy-Riemann equations (2.12) given by Proposition 35. Then u^* has the same Dirichlet energy as u, and u^* is discrete harmonic in S_h^*.*

Proof. Let u^* be the solution of the discrete Cauchy-Riemann equations (2.12) for a discrete harmonic map $u \in S_h$. Then we show that u^* is a critical point of the non-conforming Dirichlet energy in S_h^* by rewriting the Dirichlet gradient (2.11) of u^* in terms of values of u.

On a single triangle T with midpoint m_i on edge c_i, we note that

$$\left\langle J\nabla u_{|T}, \nabla\psi_i \right\rangle = \frac{2}{\operatorname{area} T}(u(m_{i-1}) - u(m_{i+1})) \;\forall i \in \{1,2,3\}, \quad (2.15)$$

which follows directly from $\nabla u = \sum_{j=1}^{3} u(m_j)\nabla\psi_j$ and

$$\left\langle J\nabla\psi_j, \nabla\psi_i \right\rangle = \begin{cases} 0 & j = i \\ \frac{2}{\operatorname{area}(T)} & j = i-1 \\ \frac{-2}{\operatorname{area}(T)} & j = i+1 \end{cases}.$$

Let $T_1 \cup T_2$ denote the two triangles forming the support of ψ_i as shown in Figure 2.4. Using Equation (2.15) we obtain

$$\begin{aligned} \frac{d}{du_i^*}E_D(u^*) &= \int_{T_1\cup T_2} \langle \nabla u^*, \nabla\psi_i \rangle \\ &= 2(u(m_{i_{-2}}) - u(m_{i_{-1}})) + 2(u(m_{i_1}) - u(m_{i_2})). \end{aligned}$$

Since u is linear we can rewrite the differences at edge midpoints as differences of u at vertices on the common edge of T_1 and T_2, and obtain

$$\frac{d}{du_i^*}E_D(u^*) = u(V_{j_{-1}}) - u(V_{j_{-2}}) + u(V_{j_2}) - u(V_{j_1}). \quad (2.16)$$

This equation relates the energy gradient of u^* to the function values at vertices of u. We emphasize the fact that the derivation of the equation does not use edge continuity of u, which will allow us to use 2.16 in the proof of Theorem 37. The right hand side of (2.16) vanishes if and only if

$$u_{|e_i \text{ in } T_1} = u_{|e_i \text{ in } T_2} + \mathit{constant}.$$

Therefore, the harmonicity of u^* follows from, and is equal to, the edge continuity of $u \in S_h$. □

The following main theorem states the complete relationship between harmonic maps in S_h and S_h^*, and includes the previous propositions as special cases.

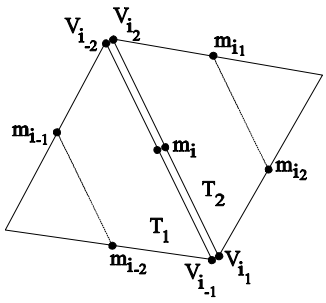

FIGURE 2.4. Notation of edge midpoints in pair of triangles.

Theorem 37 *Let M_h be a simplicial surface in $\mathbb{R}^m$ and S_h respectively S_h^* the space of conforming respectively non-conforming maps from M_h into $\mathbb{R}^d$. Then we have the following duality of Laplace-Beltrami harmonic maps on M_h:*

1. *Let $u \in S_h$ be a minimizer of the Dirichlet energy in S_h. Then its conjugate map u^* is in S_h^* and is discrete harmonic.*
2. *Let $v \in S_h^*$ be a minimizer of the Dirichlet energy in S_h^*. Then its conjugate map u is in S_h and discrete harmonic.*
3. *Let $u \in S_h$, respectively S_h^*, be discrete harmonic in S_h, respectively. S_h^*. Then $u^{**} = -u$.*

Proof. 1. The first statement was proved in Propositions 35 and 36.
2. Let $v \in S_h^*$ given by $v = \sum v_i \psi_i$ be discrete harmonic. Along the lines of the proof for the corresponding Proposition 35 concerning S_h, we define $v^*_{|T}$ (up to an additive integration constant) as the well-defined integral of

$$dv^*_{|T} := *dv_{|T} \quad \forall\, T \in M_h,$$

which uniquely exists since $v_{|T}$ is linear. Using the same arguments as in the proof of Proposition 36 and $\nabla v^* = J \nabla v$, we derive an equation for v that is identical to Equation (2.16) for u :

$$\frac{d}{dv_i} E_D(v) = v^*(V_{j_{-1}}) - v^*(V_{j_{-2}}) + v^*(V_{j_2}) - v^*(V_{j_1}),$$

where V_{j_k} are vertices as denoted in Figure 2.4. Since v is harmonic, we can choose the integration constants of v^* such that v^* becomes edge continuous and lies in S_h.

The harmonicity property of v^* follows from the closedness of v. Let $v^* = \sum v_i^* \varphi_i \in S_h$, and then splitting $\nabla\psi_i = -\nabla\psi_{i_j} - \nabla\psi_{i_{j+1}}$ in each triangle, we obtain

$$\begin{aligned}
\frac{d}{dv_i^*} E_D(v^*) &= \int_{M_h} \left\langle \nabla v^*, \frac{d}{dv_i^*} \nabla v^* \right\rangle = \int_{star(p_i)} \langle J\nabla v, \nabla \varphi_i \rangle \\
&= \sum_j \int_{T_{i_j}} \left\langle J\nabla v, -\frac{1}{2}(\nabla\psi_{i_j} + \nabla\psi_{i_{j+1}}) \right\rangle \\
&= \sum_j \int_{T_{i_j}} \frac{1}{\operatorname{area} T_{i_j}} ((v_{i_{j+1}} - v_{i_{j-1}}) + (v_{i_{j-1}} - v_{i_j})) \\
&= \sum_j v_{i_{j+1}} - v_{i_j} = 0
\end{aligned}$$

since $v \in S_h^*$ is closed on the path around each vertex p_i. Therefore v^* is critical for the Dirichlet energy in S_h.

3. The third statement is a direct consequence of applying the $*$ operator twice, which rotates the gradient in each triangle by π in the plane of the gradient. □

Corollary 38 *Conjugation is a bijection between discrete Laplace-Beltrami harmonic maps in S_h and S_h^*, where each pair (u, v) fulfills the discrete Cauchy Riemann equations. Further, corresponding maps have the same Dirichlet energy.*

Proof. The proof of Theorem 37 and the previous propositions show that, for a pair (u, v) of harmonic conjugate functions $u \in S_h$ and $v \in S_h^*$, the harmonicity condition of u is equal to the closedness condition of v, and the closedness condition of u is equal to the harmonicity condition of v.

The equality of the Dirichlet energies follows directly from the Cauchy-Riemann equations. □

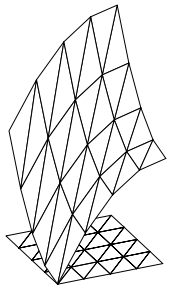

Discrete harmonic map
$u \in S_h$ interpolating $\operatorname{Re} z^2$

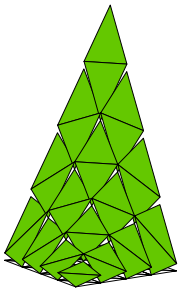

Conjugate harmonic $u^* \in S_h^*$
is a non-conforming map

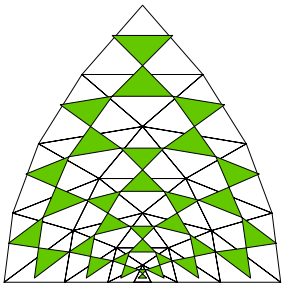

Holomorphic pair (u, u^*) and
exact solution as full grid

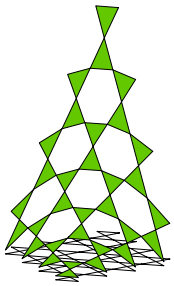

u^* applied to center
quarter of each triangle.

2.5 Minimizing with Conjugate Gradients

For completeness we will mention some of the numerical methods to practically solve the variational problems which we discussed so far. These methods apply to both the conforming and non-conforming meshes.

Let u_h be a map from a simplicial surface M_h satisfying a Dirichlet boundary value problem

$$\begin{aligned} u_h &: M_h \to \mathbb{R}^3 \\ u_{h|\partial M} &= \Gamma. \end{aligned}$$

With respect to the Lagrange basis functions, u_h is given

$$u_h(x) = \sum_{i=1}^{n} u_i \varphi_i(x).$$

Assume, we ordered the set vertices of M_h by interior and boundary vertices $\{p_1, .., p_I, p_{I+1}., p_{I+B}\}$. Then the harmonicity condition at each interior vertex p_j is

$$\begin{aligned}\frac{d}{du_j}E_D(u_h) &= \sum_{i=1}^{n} u_i \int_{M_h} \langle \nabla\varphi_i, \nabla\varphi_j \rangle \\ &= \sum_{i=1}^{I} u_i \int_{M_h} \langle \nabla\varphi_i, \nabla\varphi_j \rangle + \sum_{i=I+1}^{I+B} u_i \int_{M_h} \langle \nabla\varphi_i, \nabla\varphi_j \rangle \\ &= 0 \quad \forall\, j \in \{1, .., I\}\,.\end{aligned}$$

This system of equations is equivalent to a single matrix equation

$$Au = B$$

where $A = (a_{ji})$ is an IxI matrix, the so-called *stiffness matrix*, and $u = (u_i)$ and $B = (b_j)$ are I dimensional vectors with

$$\begin{aligned}a_{ji} &= \int_{M_h} \langle \nabla\varphi_i, \nabla\varphi_j \rangle \\ b_j &= \sum_{i=I+1}^{I+B} u_i \int_{M_h} \langle \nabla\varphi_i, \nabla\varphi_j \rangle\,.\end{aligned}$$

In praxis it is usually more efficient not solve the matrix system but employ a conjugate gradient method which is an iterative method with a fast convergence especially during the first iteration steps. See the comments of Brakke [3] who compared our method with other minimization algorithms built into the surface evolver.

The method of *steepest descent* is an iterative algorithm which incrementally reduces the energy by modifying the function u_h a small distance ε in the direction of the negative of the energy gradient

$$\begin{aligned}u_0 &: = u_h \\ u_{i+1} &: = u_i - \varepsilon \nabla E_p(u_i).\end{aligned}$$

The *conjugate gradient method* is a more efficient method where the direction vector is modified such that previous optimizations are not spoiled. It uses a sequence of *line minimizations*: given $p \in \mathbb{R}^n$, direction $n \in \mathbb{R}^n$ and an energy functional $E : \mathbb{R}^n \to \mathbb{R}$. Find a scalar λ that minimizes

$$E(p + \lambda n) \to \min,$$

and then replace p by $p + \lambda n$. If the energy functional is differentiable then an obvious choice for a direction is the gradient of E. Such a

gradient method can be more efficient by incorporating second order information which avoids spoiling of previous results.
The Taylor expansion around p gives

$$\begin{aligned} E(x) &= E(p) + \nabla E_p(x) + \frac{1}{2}\nabla^2 E_p(x,x) + \dots \\ &\approx c - bx + \frac{1}{2}x^t A x \end{aligned}$$

For a quadratic function E the gradient can be written as

$$\nabla E(x) = Ax - b.$$

How does the gradient change along some direction ν?

$$\partial_v \nabla E = A \cdot \partial_v x = Av$$

The idea of the conjugate gradient method can be summarized as follows: assume we have moved along some direction u to a minimum and now want to move along a new direction v. Then v shall not spoil our previous minimization, i.e. the change of the gradient shall be perpendicular to u:

$$0 = \langle u, \partial_v (\nabla E) \rangle = uAv$$

The vectors u and v are called *conjugate directions* which can be constructed using the following Gram-Schmidt bi-orthogonalization procedure employed in the methods of Fletcher-Reeves and Polak-Ribiere [26][34].
Let A be a positive-definite, symmetric $n \times n$ matrix. Let g_0 be an arbitrary vector, and $h_0 = g_0$. For $i = 0, 1, 2, \dots$ define the two sequences of vectors

$$\begin{aligned} g_{i+1} &= g_i - \lambda_i A h_i \\ h_{i+1} &= g_{i+1} + \gamma_i h_i, \end{aligned} \tag{2.17}$$

where λ_i respectively γ_i are chosen to obtain mutually orthogonal vectors $g_{i+1} \cdot g_i = 0$ respectively mutually conjugate directions $h_{i+1} A h_i = 0$, that is:

$$\lambda_i = \frac{g_i \cdot g_i}{g_i A h_i} \qquad \gamma_i = -\frac{g_{i+1} A h_i}{h_i A h_i}.$$

If denominators are zero take $\lambda_i = 0$ resp. $\gamma_i = 0$. Then

$$g_i \cdot g_{i+1} = 0 \qquad h_i A h_j = 0 \qquad \forall i \neq j$$

and the bi-orthogonalization procedure has produced a sequence g_i where each g_i is orthogonal and each h_i is conjugate to its set of predecessors.

Generally, the Hessian matrix A is not known. In this case the following observation provides the essential hints. Assume E is a quadratic functional and we take

$$g_i := -\nabla E|_{p_i} \quad \text{for some point } p_i.$$

Then we proceed from p_i along the direction h_i to the local minimum of E which is located at some point p_{i+1}. If we set again $g_{i+1} := -\nabla E_{|p_{i+1}}$ then this vector g_{i+1} is exactly the vector which would have been obtained by the above Equations 2.17 but without the knowledge of the Hessian A. More precisely, the matrix A never needs to be computed.

Summarizing, the conjugate gradient method computes a set of directions h_i using only line minimizations, the evaluations of the energy gradient, and an auxiliary vector to store the recent vectors g_i. In practice, further optimizations are obtained through pre-conditioning.

2.6 Discrete Laplace Operators

The discretization of the second order Laplace operator for smooth functions to simplicial meshes may be pursued in different ways. Depending on the structure of and information about the underlying mesh the Laplace operator may include more combinatorial or more geometric information. Here we review some basic combinatorial Laplacians and then relate them with the Laplace-Beltrami operator in the context of the functions spaces used in this chapter.

Combinatorial Laplacian

The purely combinatorial point of view ignores metric information like edge length or vertex angles of a mesh. All information about a combinatorial mesh is contained in its connectivity. For theoretical purposes it is convenient to express the connectivity in the form of the adjacency matrix.

Definition 39 *Let $\{p_1, ..., p_n\}$ be the vertices of a mesh. Then the* adjacency matrix *A of the mesh connectivity is an $n \times n$ matrix given*

by

$$A_{ij} = \begin{cases} 1 & \text{if } p_i p_j \text{ is an edge} \\ 0 & \text{else} \end{cases}$$

The matrix A is sparse, and the sum of the $i-$th row respectively column is equal to the valence d_i of the vertex i. Note, in practical applications one would never explicitly store the full matrix.

Definition 40 *Let D be an $n \times n$ diagonal matrix with entries $d_{ii} := \frac{1}{d_i}$ where d_i is the valence of the vertex p_i, then the matrix*

$$\begin{aligned} L &: = \mathrm{id} - DA \\ L_{ij} &= \begin{cases} 1 & i = j \\ -\frac{1}{d_i} & \text{if } p_i p_j \text{ is an edge} \\ 0 & \text{else} \end{cases} \end{aligned}$$

is the combinatorial Laplacian *of the mesh, or short, the* mesh Laplacian.

Let e_i be the vector $(0, ..0, 1, 0, .., 0)$ with 1 at the $i-$th position which is associated to p_i. Then

$$Le_i = e_i - \frac{1}{d_i} \sum_{j \in n(i)} e_j$$

where $n(i)$ denotes the set of vertices adjacent to p_i excluding p_i.
Karni and Gotsmann [19] extend the mesh Laplacian in the framework of mesh compression to include distance information

$$GL(p_i) = p_i - \frac{\sum_{j \in n(i)} \frac{1}{|p_i - p_j|} p_j}{\sum_{j \in n(i)} \frac{1}{|p_i - p_j|}}.$$

Five-Point Laplacian

The five-point Laplacian is the $2d-$extension of the finite difference Laplacian on the real axis. Consider a real-valued function $f : \mathbb{R} \to \mathbb{R}$ on an interval of the real axis. Then the smooth Laplacian Δf is defined as second derivative of f. In the discrete case, let $\{u_i\}$ be a uniform knot vector on the axis, for example, $u_i := i$, then $f_h"(x_i)$ can be approximated using finite differences

$$\begin{aligned} f_h"(x_i) &= \frac{1}{2} \left(f_h'(x_i) - f_h'(x_i) \right) \\ &= \frac{1}{2} \left((f(x_{i+1}) - f(x_i)) - (f(x_i) - f(x_{i-1})) \right) \\ &= \frac{1}{2} \left(f(x_{i+1}) - 2f(x_i) + f(x_{i-1}) \right) \end{aligned}$$

This can be written in matrix representation

$$\Delta f_h = -Af_h$$

with $f = (f(x_0), f(x_1), ..)$ and the matrix

$$A = \frac{1}{2}\begin{pmatrix} 0 & & & & & & & & \\ -1 & 2 & -1 & & & & & & \\ & -1 & 2 & -1 & & & & & \\ & & & .. & & & & & \\ & & & & .. & -1 & 2 & 1 & \\ & & & & & & & & 0 \end{pmatrix}.$$

A smoothing operation of f can be performed by a so-called Gaussian filtering method

$$f_h^{j+1} := f_h^j + \lambda \Delta f_h^j$$

with a scalar factor $0 < \lambda < 1$. Other values of λ will enhance the variation of f. In matrix form we have

$$f_h^{j+1} = f_h^j - \lambda A f_h^j$$

Discrete Laplace-Beltrami Operator on Surfaces

Let M_h be a simplicial surface in $\mathbb{R}^m$. We now define the Laplace operator for piecewise linear functions in S_h respectively S_h^* similar to the derivation of the discrete Dirichlet energy. Since second derivatives are involved the discrete Laplace-Beltrami operator will be a function on the vertices respectively edge midpoints, and it will not extend as a piecewise linear function over the whole triangulation.

Definition 41 *Let $u \in S_h$ be a map $u : M_h \to \mathbb{R}^d$ on a simplicial surface M_h with set of vertices V_h. Then the (total)* discrete Laplacian *$\Delta_h u(p) \in \mathbb{R}^d$ at each vertex $p \in V_h$ is defined as*

$$\Delta_h u(p) := -\int_{\text{star } p} \langle \nabla u, \nabla \varphi_p \rangle . \tag{2.18}$$

Similarly, let $u \in S_h^*$ be a non-conforming map then $\Delta_h^* : S_h^* \to V_h^*$ at an edge midpoint m is given by

$$\Delta_h^* u(m) := -\int_{\text{star } m} \langle \nabla u, \nabla \psi_m \rangle \tag{2.19}$$

with basis functions $\varphi_p \in S_h$ and $\psi_m \in S_h^*$.

In explicit notation we have at an interior vertex p and an interior edge midpoint m

$$\begin{aligned}\Delta_h u(p) &= -\frac{1}{2}\sum_{q_i \in n(p)} (\cot\alpha_i + \cot\beta_i)(u(p) - u(q_i)) \\ \Delta_h^* u(m) &= -2(\cot\alpha_{-2}(u(m) - u(m_{-1})) + \cot\alpha_{-1}(u(m) - u(m_{-2})) \\ &\quad + \cot\alpha_1(u(m) - u(m_2)) + \cot\alpha_2(u(m) - u(m_1)))\end{aligned}$$

where $\{q_i\}$ is the set of vertices on the link of p, and $\{m_i\}$ the set of vertices on the link of m in counter-clockwise order and vertex angles α_i opposite to m_i in each triangle.

3

Discrete Minimal Surfaces

Minimal surfaces are characterized by having least area compared to nearby surfaces with the same boundary. This variational property, which was the original interest in minimal surfaces, was soon relaxed to include unstable critical points as well. Equivalently, these surfaces can be geometrically characterized by having vanishing mean curvature.

Examples have played a central part in the development of the minimal surface theory and fruitfully complemented the theoretical research. In recent years many new examples were studied experimentally using elaborate calculations for the analytic continuation of complex functions and the integration of the Weierstraß representation formulas. Although these methods allow one to compute any surface given by its Weierstraß representation, this analytic approach has the drawback that the Weierstraß formulas must be known in advance. Since the existence of many unstable minimal surfaces was mathematically proved indirectly via the so-called *conjugate surface construction* there was a strong need to develop a numerical scheme and actually compute the conjugate surface of a minimal surface [17][18].

The numerical method developed in [25] jointly with Pinkall was the first scheme to compute the conjugate of a numerically computed minimal surface. The key insight came from a new understanding of the geometric and variational properties of triangle nets. The method

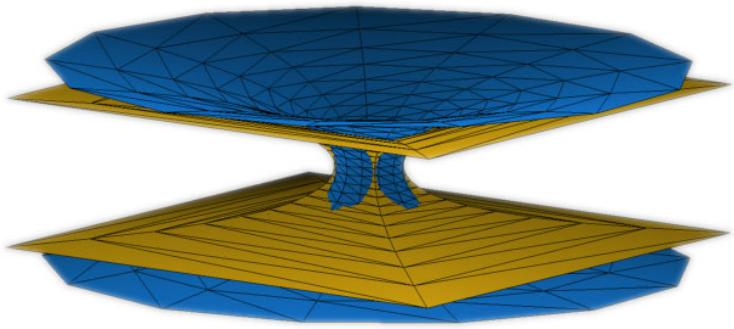

FIGURE 3.1. Asymptotic growth of two complete discrete catenoids depends on the dihedral symmetry.

was later extended in [23] jointly with Oberknapp to the computation of constant mean curvature surfaces via a conjugation of minimal surfaces in $\mathbb{S}^3$.

The main theoretical result in this section is a new precise understanding of the variational properties of pairs of discrete conjugate minimal surfaces, which was not known in the original works, by working in the function space of non-conforming triangle meshes. This chapter also introduces discrete minimal surfaces and derives their variational properties, we define the mean curvature normal as an operator on the discrete mesh.

Another important result is an explicit description of some complete discrete minimal surfaces which were jointly discovered with Rossman [32]. For example, these descriptions allow one to construct unstable discrete surfaces whose shape is given by exact coordinates, a fact which is particularly useful for the study of higher order properties like the index of minimal surfaces.

3.1 Review of the Smooth Variation of Area

Let $F : \Omega \to M \subset \mathbb{R}^3$ be a parameterized surface of a domain $\Omega \subset \mathbb{R}^2$. A variation of M is a family of surfaces given by a differentiable map

$$\begin{aligned} G : \Omega \times (-\varepsilon, \varepsilon) &\to \mathbb{R}^3 \\ G(x, 0) &= F(x) \quad x \in \Omega. \end{aligned}$$

The induced vector field on M

$$\begin{aligned} Y &: \Omega \to TM \\ Y(x) &= \frac{d}{d\varepsilon} G(x,\varepsilon)_{|\varepsilon=0} \end{aligned}$$

is called the *first variation* of G.

Lemma 42 *For a given surface M and a variation vector field Y the first variation of the area functional at M in the direction of Y is defined by*

$$\delta \operatorname{area}(M,Y) := \frac{d}{d\varepsilon} \operatorname{area}(M_\varepsilon)_{|\varepsilon=0} \in \mathbb{R}$$

and given by

$$-\delta \operatorname{area}(M,Y) = \int_{\partial M} \langle Y, \nu \rangle \, ds + 2 \int_M \langle Y, N \rangle \, H dA \ ,$$

where ν is the outer normal along ∂M.

Proof. *see Hildebrandt et al. [6] or Lawson [16].* □

If $Y = \lambda N$ is a normal variation then the boundary component vanishes and we have

$$\delta \operatorname{area}(M,Y) = -2 \int_M \lambda H dA.$$

Further, if $\lambda \equiv 1$ and H is constant we obtain

$$H = -\frac{\delta \operatorname{area}(M,N)}{\operatorname{area}(M)}.$$

3.2 First Variation of the Discrete Area and Volume

A variation of a polyhedral surface is determined by a variation of its vertices with the same mesh connectivity. For simplicity we require a C^2 variation but often a differentiability of lower order is sufficient.

Definition 43 *Let $\mathcal{P} = \{p_1, ..., p_m\}$ be the set of vertices of a discrete surface M_h. A* variation *$M_h(t)$ of M_h is defined as a C^2 variation of the vertices p_i*

$$p_i(t) : [0, \epsilon) \to \mathbb{R}^d \quad \text{so that} \quad p_i(0) = p_i \ \forall i = 1, .., m.$$

The straightness of the edges and the flatness of the triangles are preserved as the vertices move.
Formally, we have for each t that $p_i(t) \in S_h$ and $p_i(0) = id(M_h)$ is the identity map of M_h.

Up to first order a variation is given by a set of vectors $\mathcal{V} = \{v_1, ..., v_m\}$, $v_i \in \mathbb{R}^d$ defined on the vertices $\mathcal{P} = \{p_1, ..., p_m\}$ of M_h. Often we restrict a variation to interior vertices by assuming $v_i = 0 \in \mathbb{R}^d$ along the boundary, or add special constraints on the boundary of M_h. The vectors v_{p_j} are the *variation vector field* such that the variation has the form

$$p_j(t) = p_j + t \cdot v_{p_j} + \mathcal{O}(t^2), \tag{3.1}$$

that is, $p_j'(0) = v_{p_j}$. We define the vector $\vec{v} \in \mathbb{R}^{dm}$ by

$$\vec{v^t} = (v_1^t, ..., v_m^t). \tag{3.2}$$

In the following we will restrict to $d = 3$ which allows the use of a well-defined normal vector although many results hold in higher codimension too.
In the smooth situation, the variation at interior points is typically restricted to normal variation since the tangential part of the variation only performs a reparametrization of the surface. However, on discrete surfaces there is an ambiguity in the choice of normal vectors at the vertices, so we allow arbitrary variations.
In the following we derive the evolution equations for some basic discrete operators under variation $M_h(t)$ of a discrete surface M_h.
Recalling, that the area of a discrete surface is

$$\operatorname{area} M_h := \sum_{T \in \mathcal{T}} \operatorname{area} T,$$

where $\operatorname{area} M_h$ denotes the Euclidean area of the triangle T as a subset of $\mathbb{R}^3$.
At each vertex p of M_h, the gradient of area is

$$\nabla_p \operatorname{area} M_h = \frac{1}{2} \sum_{T=(p,q,r) \in \operatorname{star} p} J(r - q), \tag{3.3}$$

where J is rotation of angle $\frac{\pi}{2}$ in the plane of each oriented triangle T. The first derivative of the surface area is then given by the chain rule

$$\frac{d}{dt} \operatorname{area} M_h = \sum_{p \in \mathcal{V}} \langle p', \nabla_p \operatorname{area} M_h \rangle. \tag{3.4}$$

The volume of an oriented surface M_h is the oriented volume enclosed by the cone of the surface over the origin in $\mathbb{R}^3$

$$\operatorname{vol} M_h := \frac{1}{6} \sum_{T=(p,q,r)\in M_h} \langle p, q \times r \rangle = \frac{1}{3} \sum_{T=(p,q,r)\in M_h} \langle \vec{N}, p \rangle \cdot \operatorname{area} T,$$

where p is any of the three vertices of the triangle T and $\vec{N} = (q - p) \times (r - p)/|(q - p) \times (r - p)|$ is the oriented normal of T. It follows that

$$\nabla_p \operatorname{vol} M_h = \sum_{T=(p,q,r)\in \operatorname{star} p} q \times r/6 \tag{3.5}$$

and

$$\frac{d}{dt} \operatorname{vol} M_h = \sum_{p\in\mathcal{P}} \langle p', \nabla_p \operatorname{vol} M_h \rangle. \tag{3.6}$$

Remark 44 *Note also that* $\nabla_p \operatorname{vol} M_h = \sum_{T=(p,q,r)\in \operatorname{star} p} (2 \cdot \operatorname{area} T \cdot \vec{N} + p \times (r - q))/6$. *Furthermore, if* p *is an interior vertex, then the boundary of* $\operatorname{star} p$ *is closed and* $\sum_{T\in \operatorname{star} p} p \times (r - q) = 0$. *Hence the* $q \times r$ *in Equation 3.5 can be replaced with* $2 \cdot \operatorname{area} T \cdot \vec{N}$ *whenever* p *is an interior vertex.*

3.3 Discrete Mean Curvature

The mean curvature vector on smooth surfaces provides a measure how much the surface area changes compared to near-by surfaces, that means, if a surface is moved at constant speed along the surface normal. In the polyhedral case we will use a similar approach to obtain a discrete version of the mean curvature vector. Similar to the definition of a discrete Gauß curvature the polyhedral mean curvature will measure the curvature of a small region. Later it will turn out that the mean curvature vector can be interpreted as the discrete Laplace-Beltrami operator on surfaces which was introduced in Section 2.

The area of a polyhedral surface is defined as the sum of the area of all elements. Let T be a triangle spanned by two edges v and w emanating from a vertex then its area is given by the relation $4 \operatorname{area}^2 T = |v|^2 |w|^2 - \langle v, w \rangle^2$. In the following we prefer an expression of the area in terms of vertices and vertex angles of the surface. Let T be a triangle with vertices q_i and vertex angles α_i. Then

$$\operatorname{area} T = \frac{1}{4} \sum_{j=1}^{3} \cot \alpha_j \, |q_{j-1} - q_{j+1}|^2 . \tag{3.7}$$

For practical applications we derive a simple formula of the area gradient in intrinsic terms of the polyhedral mesh, see [25].

Lemma 45 *Let p be an interior vertex of a simplicial surface M_h. Then the gradient of the area with respect to variation of vertices can be expressed in the following cotangent formula*

$$\nabla_p \operatorname{area} M_h = \frac{1}{2} \sum_j (\cot \alpha_j + \cot \beta_j)(p - q_j). \tag{3.8}$$

Proof. The area gradient is the sum of the individual area gradients of all triangles containing p. In each triangle the area gradient of p is parallel to the height vector point toward p with length $|c|$. If c is the oriented edge opposite to p and J the rotation in the oriented plane of the triangle by $\frac{\pi}{2}$ then the gradient can be expressed by $\frac{1}{2}Jc$. Summing over all triangles containing p we obtain

$$\nabla_p \operatorname{area} M_h = \frac{1}{2} \sum_j Jc_i.$$

Using the explicit representation of Jc on a single triangle with edges $c = a - b$ and vertex angles α and β at the end points of c,

$$Jc = a \cot \alpha + b \cot \beta,$$

one obtains the proposed equation. □

This formula easily generalizes to non-manifold surfaces where, for example, three triangles join at a common edge.

If $M_h(t)$ is a variation of simplicial surfaces such that each vertex $p(t)$ is a differentiable function for $t \in (-\varepsilon, \varepsilon)$ then

$$\frac{d}{dt} \operatorname{area} M_h(t) = \sum_{p \in P} \langle p', \nabla_p \operatorname{area} M_h \rangle .$$

The mean curvature of a smooth surface measures the variation of area when changing to parallel surfaces in normal direction. In the discrete case there exists no unique normal vector, but, as first derived in [25], if we choose as normal vector the direction of the area gradient, then the following definition leads to a discrete mean curvature vector which has similar properties as the smooth mean curvature vector.

Definition 46 *The discrete mean curvature at the vertex p of a simplicial surface M_h is a vector-valued quantity*

$$\overrightarrow{H}(p) := \nabla_p \operatorname{area} M_h. \tag{3.9}$$

Note that this mean curvature operator is an integrated operator and measures the total mean curvature in the vicinity of a vertex. Therefore, when computing the total mean curvature of a surface one simply needs to sum up the mean curvature of all vertices instead of integrating over the surface. In this sense, the mean curvature is a measure at vertices similar to the (total) Gauss curvature introduced in [33]. This constrasts to the use of non-total discrete mean curvatures in [13] in the experimental study of minimizers of the Willmore integral.

3.4 Properties of Discrete Minimal Surfaces

In the previous section we have introduced the notion of mean curvature vector as the gradient of the discrete area functional. Here we will study the critical values of the area functional in more detail, that is, surfaces with $H \equiv 0$.

Definition 47 *A simplicial surface M_h is a* discrete minimal surface *iff the discrete area functional of M_h is critical w.r.t. variations of any set of interior vertices. To include symmetry properties into this definition we sometimes allow a constrained variation of boundary points:*

- *if a boundary arc is a straight line, then its interior points may vary along the straight line*
- *if a boundary arc is a planar curve, then its interior points may vary within the plane*
- *in all other cases the boundary points always remain fixed.*

Note that the above definition is equivalent to saying that the area of M_h is critical with respect to variations of any interior vertex. The relaxed boundary constraints allow us to simulate free boundary value problems, and to extend minimal surfaces by reflection.

Corollary 48 *A simplicial surface M_h is minimal if and only if at each interior vertex p*

$$\nabla_p \operatorname{area} M_h = \frac{1}{2} \sum_j (\cot \alpha_j + \cot \beta_j)(p - q_j) = 0 \tag{3.10}$$

where $\{q_j\}$ denotes the set of vertices of $\operatorname{link} p$ *and α_j,β_j denote the two angles opposite to the edge pq_j. At boundary vertices on symmetry*

arcs the area gradient is constraint to be tangential to the straight line or to the plane.

Proof. This equation follows directly from the representation of the area gradient as the discrete mean curvature vector. □

The following properties of discrete minimal surfaces derived in [25] are similar to equivalent properties of harmonic maps.

Lemma 49 *Let M_h be a discrete minimal surface. If the star of an interior vertex p consists of congruent isosceles triangles then p lies in the center of mass of the vertices of its link.*

Proof. The weights in Equation 3.10 are all equal, therefore, p is the mean of its adjacent vertices $\{q_i\}$. □

The convex hull property for discrete minimal surfaces holds as long as the surface consists only of acute triangles.

Lemma 50 *Let M_h be a discrete minimal surface. If the star of an interior vertex p consists of acute triangles then p lies in the convex hull of its star.*

Proof. The weights in Equation 3.10 are all positive, therefore, p is a convex combination of its adjacent vertices $\{q_i\}$

$$p = \frac{\sum_j (\cot \alpha_j + \cot \beta_j) q_j}{\sum_j (\cot \alpha_j + \cot \beta_j)}$$

and lies within the convex hull of its link spanned by $\{q_i\}$. □

The previous lemma does not hold in a more general case. The following configuration is a counterexample to the maximum principle and the convex hull property of discrete minimal surfaces. Its construction in [32] jointly with Rossman is based on the existence of obtuse triangles. See also the model at [30] which contains an interactive applet to analyze the dependence on the boundary configuration.

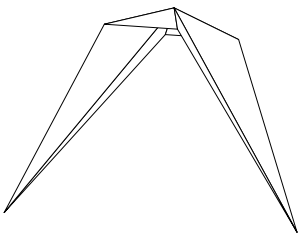

Counterexample to the maximum principle of discrete minimal surfaces. The center vertex lies outside the convex hull of its link.

The counterexample is a special configuration of the 1−parameter family of discrete minimal surfaces:

<points>
-u 0 -u
 u 0 -u
-1 1 0
 1 1 0
-1 -1 0

```
    <p> 1 -1 0 </p>
    <p> 0 0 h(u)</p>
</points>
<faces>
    <f>0 6 2</f>
    <f>6 3 2</f>
    <f>6 1 3</f>
    <f>0 4 6</f>
    <f>4 5 6</f>
    <f>5 1 6</f>
</faces>
```

The parameter u varies in $(0, \infty)$ and the function $h(u)$ determines the vertical height of the center vertex. For $u \in [0, 2]$ the central vertex lies within the convex hull of the boundary after minimization. The remarkable fact is that this property does not hold for $u > 2$ when the minimum position of the central vertex is outside the convex hull of the boundary. The model in the margin figure corresponds to the parameter value $u = 5$.

Note that since the identity map of a discrete minimal surface is a discrete harmonic map, this example also demonstrates that the mean value property and convex hull property of discrete harmonic maps do not hold. Further note that both properties hold in special situations where all triangles have all vertex angles in $[-\frac{\pi}{2}, \frac{\pi}{2}]$. In this example, the center vertex lies on the convex hull exactly at $u = 2$ which is the situation when the first vertex angle becomes $\frac{\pi}{2}$. Increasing u further leads to an increasing angle.

Note that the discrete maximum principle does hold for the five-vertex Laplacian defined over the special rectangular $\mathbb{Z} \times \mathbb{Z}$ grid [4].

3.5 Computing Discrete Minimal Surfaces

A direct minimization of the area functional is a non-linear problem because of the angle terms in Equation 3.10. Another effect, which may spoil numerical convergence, is the invariance of the area functional with respect to reparametrizations of the image surface. This may lead to tangential motions in an area minimization procedure.

The following observation leads to an effective method for area minimization which in fact minimizes the Dirichlet energy in an iteration process. This method was first employed by Dziuk [7] for the mean

curvature flow and later used in the context of discrete minimal surfaces by Pinkall and Polthier [25]. For a smooth map $F : M \to \mathbb{R}^3$ from a Riemann surface M we have the estimate

$$\operatorname{area} F(M) \leq \frac{1}{2} \int_M |\nabla F|^2 \, dx =: E_D(F)$$

with equality iff F is a conformal map. Following a proposal of Hutchinson [15] we call the difference

$$E_C(F) := E_D(F) - \operatorname{area} F(M)$$

the *conformal energy* of the map F since for a Euclidean (x, y)-domain Ω one has

$$E_C(F) = \frac{1}{2} \int_\Omega |JF_x - F_y|^2 , \tag{3.11}$$

where J is the rotation by $\frac{\pi}{2}$ in the oriented tangent plane. E_C is a natural measure of failure for a map to be conformal. In the following we will introduce a discrete analogue of these relationships.

Lemma 51 *The gradient of the Dirichlet energy of the identity map* id *of a simplicial surface M_h is equal to the area gradient, that is, at any interior vertex $p \in M$ we have*

$$\nabla_p \operatorname{area} M_h = \nabla_p E_D(\mathrm{id}).$$

Proof. The statement follows directly by applying the theorem 20 to the id map and comparing its Dirichlet gradient with the area gradient of M_h. □

Corollary 52 *A simplicial surface M_h is minimal if and only if the identity map* $\mathrm{id}_h : M_h \to M_h$ *is discrete harmonic.*

As a consequence, we have a simplicial equivalent for the conformal energy of smooth maps given in Equation 3.11.

Definition 53 *Let $F_h : M_h \to N_h$ be a map between two simplicial surfaces, then its discrete conformal energy is given by*

$$E_C(F_h) := E_D(F_h) - \operatorname{area} F_h(M_h). \tag{3.12}$$

Corollary 54 *Let $F_h : M_h \to N_h$ be a map between two simplicial surfaces, then the discrete conformal energy and its gradient are*

$$E_C(F_h) = \frac{1}{4} \sum_{p_i p_j \text{ is edges}} (\Delta\alpha_{ij} + \Delta\beta_{ij}) \, |F_h(p_i) - F_h(p_j)|^2$$

$$\nabla_{F_h(p_i)} E_C(F_h) = \frac{1}{2} \sum_{p_j \in \text{link } p_i} (\Delta\alpha_{ij} + \Delta\beta_{ij})(F_h(p_i) - F_h(p_j)) \quad (3.13)$$

with the shortcuts

$$\begin{aligned} \Delta\alpha_{ij} &: = \cot\alpha_{ij} - \cot\overline{\alpha_{ij}} \\ \Delta\beta_{ij} &: = \cot\beta_{ij} - \cot\overline{\beta_{ij}} \end{aligned}$$

where α, β denote vertex angles on M_h and $\overline{\alpha}, \overline{\beta}$ denote vertex angles on N_h in triangles opposite to the edge $p_i p_j$.

Proof. The relations follow immediately from the expressions of the discrete area in equation 3.7

$$\nabla_{F_h(p_i)} \operatorname{area} F_h(M_h) = \frac{1}{2} \sum_{p_i p_j \text{ is edges}} \left(\cot\overline{\alpha_{ij}} + \cot\overline{\beta_{ij}}\right) (F_h(p_i) - F_h(p_j))$$

and the Dirichlet energy in Theorem 20

$$\nabla_{F_h(p_i)} E_D F_h(M_h) = \frac{1}{2} \sum_{p_i p_j \text{ is edges}} \left(\cot\alpha_{ij} + \cot\beta_{ij}\right) (F_h(p_i) - F_h(p_j)) .$$

□

Note, a map has vanishing conformal energy if and only if angles of domain and image triangles are equal. But critical values of the conformal energy are much less constrained. For example, Hutchinson [15] noticed that minimizing the conformal energy leads to nice triangulations since it avoids decreasing the surface area which occurs when minimizing the Dirichlet energy.

The following algorithm uses a sequence of discrete harmonic maps. In short, let M_0 be an initial simplicial surface and let a sequence of simplicial surfaces $\{M_i\}$ be defined as images of a sequence of maps

$$\begin{aligned} F_i &: M_i \to M_{i+1} \\ \Delta_h F_i &= 0 \\ \partial F_i(M_i) &= \Gamma \end{aligned}$$

which are discrete harmonic on M_i. If the limit surface $M := \lim M_i$ exists then the limit function $F : M \to M$ is harmonic and conformal, therefore, $F(M)$ is minimal.

The algorithm makes essential use of the fact that minimizing the Dirichlet energy also minimizes the surface area in first order. The major advantages of minimizing the Dirichlet energy compared to

minimizing surface are, first, that the minimization process has a unique solution, and, second, that tangential motions can be ignored during the first iterations. Compare the comments of Brakke on this issue [3].

Algorithm 55 *Solve the boundary value problem for discrete minimal surfaces (either Dirichlet or Neumann conditions):*

1. *Choose an arbitrary initial surface M_0 with boundary $\partial M_0 = \Gamma$ as the first approximation of M, set i to 0.*

2. *Let M_i be a surface with boundary Γ, then compute the surface M_{i+1} as minimizer of the Dirichlet energy*

$$\int_{M_i} |\nabla(F_i : M_i \to M_{i+1})|^2 = \min_{M,\partial M=\Gamma} \int_{M_i} |\nabla(F : M_i \to M)|^2 .$$

   This uniquely defines a Laplace-Beltrami harmonic function F_i whose image $F_i(M_i) = M_{i+1}$ will be taken as the domain surface in the next iteration.

3. *Set i to $i + 1$ and continue with step 2, for example, until $|\text{area}\, M_i - \text{area}\, M_{i+1}| < \epsilon$.*

In practice, this algorithm converges very quickly during the first iteration steps. It slows down if the surface is close to a critical point of the area functional probably because then the area gradient no longer approximates a "good" surface normal. In any case, if the algorithm converges to a non-degenerated surface then the limit is discrete minimal. The next convergence statement shown in [25] is merely a theoretical observation, rather than having use in practical applications since the degeneracy assumption can hardly be ensured in advance.

Proposition 56 *The algorithm converges to a solution of the problem, if no triangles degenerate.*

Proof. The condition "no triangles degenerate" means that we assume all triangle angles for all surfaces of the sequence to be uniformly bounded away from 0 and π. From the construction the sequences $\{\text{area}\, M_i\}$ and$\{E_D(F_i : M_i \to M_{i+1})\}$ are monotone decreasing:

$$\begin{aligned} \text{area}\, M_i = E_D(id_{|M_i}) &\geq E_D(F_i : M_i \to M_{i+1}) \\ &= \text{area}\, M_{i+1} + E_C(F_i) \\ &\geq E_D(id_{|M_{i+1}}) = \text{area}\, M_{i+1}. \end{aligned}$$

If no triangles degenerate we minimize in a compact set of surfaces. Therefore, a subsequence of $\{M_i\}$ converges uniformly to a limit surface M with respect to the norm assumed in the space of surfaces.

Since the identity map of the limit surface M is discrete harmonic the area gradient of M vanishes everywhere, and that means M is discrete minimal. □

Other Methods for Solving the Plateau Problem

The Plateau problem looks for a minimal surface M spanned by a given boundary curve $\Gamma \subset \mathbb{R}^3$. As an overview we mentioned three popular methods to compute a numerical solution.

Minimal graph: If the surface is known to be a graph over a plane, then there exists a scalar valued function z over a planar domain $\Omega \subset \mathbb{R}^2$ with boundary $\partial\Omega$

$$\begin{aligned} z &: \Omega \to \mathbb{R} \\ z_{|\partial\Omega} &= g_1 \text{ or} \\ \partial_v z_{|\partial\Omega} &= g_2 \end{aligned}$$

where g_1 are prescribed Dirichlet boundary values, or g_2 are Neumann boundary conditions which prescribe the directional derivative of z in direction of the outer normal along $\partial\Omega$. Such a graph is area minimizing w.r.t. to variations with compact support if it fulfills a nonlinear elliptic partial differential equation, the minimal surface equation [6]

$$(1 + z_y^2)z_{xx} - 2z_x z_y z_{xy} + (1 + z_x^2)z_{yy} = 0$$

Mean curvature flow allows us to gradually decrease surface area. Let $M(t)$ with $\partial M(t) = \Gamma$ be a 1-parameter family of C^2 surfaces which is differentiable in t. Then $M(t)$ flows by mean curvature if it fulfills the following parabolic partial differential equation

$$\frac{\partial}{\partial t} M(t) = H(t) \cdot N(t) = \Delta_g M$$

where $H(t)$ is the mean curvature and $N(t)$ the surface normal of $M(t)$. If the flow does not run into a singularity and if it stops, then this limit surface is minimal.

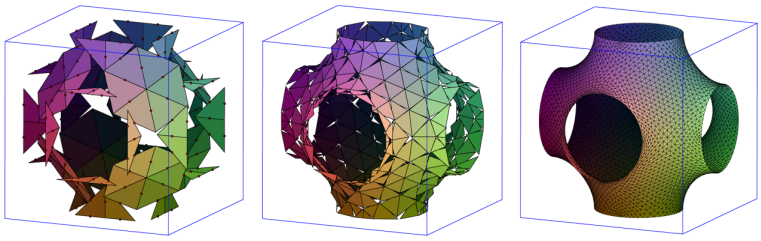

FIGURE 3.2. Free-boundary value problem of Schwarz P-surface in a cube solved via discrete conjugate surface construction. Even the very coarse resolution of the non-conforming mesh gives qualitatively good results.

3.6 Conjugate Pairs of Discrete Minimal Surfaces

Here we combine the results on non-conforming meshes of Section 2 and on simplicial minimal surfaces to derive the variational properties of pairs of conjugate discrete minimal surfaces.

Review of Smooth Minimal Surfaces

Among the fundamental observations in the theory of smooth minimal surfaces was the fact that each minimal surface comes in a family of minimal surfaces, the so-called *associate family* or *Bonnet family*. The simplest and most known example is the associate family which transforms the catenoid C into the helicoid H, both are given by

$$C(u,v) = \begin{pmatrix} \cos v \cosh u \\ \sin v \cosh u \\ u \end{pmatrix}, \qquad H(u,v) = \begin{pmatrix} \sin v \sinh u \\ -\cos v \sinh u \\ v \end{pmatrix}.$$

Their associate family $F^\varphi(u,v)$ consists of all minimal surfaces given by

$$F^\varphi(u,v) = \cos\varphi \cdot C(u,v) + \sin\varphi \cdot H(u,v).$$

The surface $F^{\frac{\pi}{2}}$ is called the *conjugate surface* of F^0, and more general, all pairs F^φ and $F^{\varphi+\frac{\pi}{2}}$ are conjugate to each other. Applying the conjugate twice leads to $F^\pi = -F$ which is obtained from F^0 by reflection in the origin.

A more appropriate notation of the associate family follows from the representation of minimal surfaces as complex curves in $\mathbb{C}^3$. Recall the basic fact in minimal surface theory that the three coordinate functions $F = (f_1, f_2, f_3)$ of a minimal surface $F : \Omega \subset \mathbb{R}^2 \to \mathbb{R}^3$

are harmonic maps if F is a conformal parameterization. Therefore, there exist three conjugate harmonic maps f_i^* which describe another minimal immersion $F^* = (f_1^*, f_2^*, f_3^*) : \Omega \subset \mathbb{R}^2 \to \mathbb{R}^3$. If we introduce complex coordinates $z = u + iv$ in Ω then combination of both maps to a holomorphic curve $F + iF^* : \Omega \to \mathbb{C}^3$ with holomorphic coordinate functions gives a family of immersions.$F^\varphi = \mathrm{Re}(e^{-i\varphi} \cdot (F + iF^*)$ called the associate family of F or of F^*. In the above example the introduction of complex coordinates leads to the following representation of the associate family of catenoid and helicoid given by

$$F^\varphi(z) = \mathrm{Re}(e^{-i\varphi} \cdot (C(z) + i \cdot H(z))) = \mathrm{Re}(e^{-i\varphi} \cdot \begin{pmatrix} \cosh z \\ -i \sinh z \\ z \end{pmatrix}).$$

The following theorem summarizes the most important properties of the associate family of smooth minimal surfaces without proof.

Theorem 57 *Let $C, H : \Omega \to \mathbb{R}^3$ be a pair of conformally parametrized conjugate minimal surfaces. Then the associate family $F^\varphi : \Omega \to \mathbb{R}^3$ has the following properties:*

1. *All surfaces F^φ of the associate family are minimal and isometric.*

2. *The surface normal at each point $F^\varphi(u, v)$ is independent of φ.*

3. *The partial derivatives fulfill the following correspondence:*

$$\begin{aligned} F_u^\varphi(u,v) &= \cos\varphi \cdot C_u(u,v) - \sin\varphi \cdot C_v(u,v) \\ F_v^\varphi(u,v) &= \sin\varphi \cdot C_u(u,v) + \cos\varphi \cdot C_v(u,v) \end{aligned},$$

   in particular, the partials of a conjugate pair C and H satisfy the Cauchy-Riemann equations:

$$\begin{aligned} C_u(u,v) &= H_v(u,v) \\ C_v(u,v) &= -H_u(u,v) \end{aligned}.$$

   This relation can be written in a compact form $dH = *dC$ using the Hodge $*$ operator.

4. *If a minimal patch is bounded by a straight line, then its conjugate patch is bounded by a planar symmetry line and vice versa. This can be seen in the catenoid-helicoid examples, where planar meridians of the catenoid correspond to the straight lines of the helicoid.*

5. *Since at every point the length and the angle between the partial derivatives are identical for the surface and its conjugate (i.e. both surfaces are isometric) we have as a result, that the angles at corresponding boundary vertices of surface and conjugate surface are identical.*

The last two properties are most important for the later conjugate surface method.

Review of the Conjugate Surface Construction

Over the last decade the conjugate surface method has been established as one of the most powerful techniques to construct new minimal surfaces with a proposed shape in mind. One of the major drawbacks of the method is the so-called period problem which often prevents a rigorous existence proof of the examples. In these situation where theoretical techniques fail up to now, a numerical approach is required to allow experiments.

The major obstacle for a numerical simulation of the conjugate surface method is the fact, that the minimal surfaces are usually unstable. Currently, the conjugation method based on discrete minimal surfaces is the only numerical method to compute the conjugate of a polyhedral minimal surface with satisfactory results.

3.6.1 Discrete Conjugate Minimal Surface

In this section we develop the notion of the conjugate and the associate family of a discrete minimal surface. In [25] the discrete conjugation algorithm is based the concept of discrete harmonic maps, but the method did not unveil the variational properties of the conjugate surface. In the following we first show the area minimality of the conjugate discrete minimal surface, and second, describe a practical algorithm by reformulating the conjugation method of [25] in terms of the conjugation of harmonic maps using conforming and non-conforming functions derived in Section 2.

Currently, the method [25] seems to be the only method to allow the conjugation of a numerically computed discrete minimal surface with reasonable results. The main difficulties are to provide accurate C^1 information, which is required for the conjugation, from numerically obtained minimal surfaces.

The remaining part of this section shows that the conjugate minimal surface is well-defined, and derives some important properties. Most

results follow from properties of the conjugate harmonic coordinate functions.

Let us review some properties of the differential of a polyhedral map $F : M_h \to \mathbb{R}^d$ where either $F \in S_h$ or $F \in S_h^*$. At each point $p \in M_h$ the differential $\nabla_p F : T_p M_h \to T_{F(p)} F(M_h)$ is given by

$$\nabla_p F(v) = \begin{pmatrix} \langle \nabla_p f_1, v \rangle \\ .. \\ \langle \nabla_p f_d, v \rangle \end{pmatrix} \quad \forall\, v \in T_p M_h$$

if $F = (f_1, .., f_d)$ are the coordinate functions. A map F is said to be harmonic if all coordinate functions are harmonic with respect to the metric of M_h. Recalling the definition of the Hodge $*$ operator directly leads to the following definition by applying the operator on the component functions. We say that a simplicial surface M_h is in S_h respectively S_h^* if the triangulation is edge continuous respectively edge-midpoint continuous.

Definition 58 *Let $F = (f_1, .., f_d) : M_h \to \mathbb{R}^d$ be a simplicial map in S_h or S_h^*. The Hodge star operator is defined by*

$$*dF_{|p}(v) := \begin{pmatrix} *df_{1|p}(v) \\ .. \\ *df_{d|p}(v) \end{pmatrix} = \begin{pmatrix} \langle J\nabla_p f_1, v \rangle \\ .. \\ \langle J\nabla_p f_d, v \rangle \end{pmatrix} \; \forall\, v \in T_p M_h$$

where J is the rotation by $\frac{\pi}{2}$ in the oriented tangent space of each triangle of M_h with respect to the metric in M_h.

For example, if $F = \mathrm{id} : M_h \to M_h$ is the identity map of a simplicial surface, then we obtain on each triangle

$$*d\,\mathrm{id}_{|p}(v) := -Jv \;\forall\, v \in T_p M_h. \tag{3.14}$$

Now we are ready to extend the results on discrete harmonic maps of the previous section to the conjugation of simplicial minimal surfaces. In the following theorem we show that the differential $*d\,\mathrm{id}$ is closed on simplicial minimal surfaces, and that its integral gives the conjugate minimal surface:

Definition 59 *Let M_h be a simplicial minimal surface in S_h (or in S_h^*). Then a* discrete conjugate minimal surface *M_h^* is a solution of Equation 3.14.*

The following theorem justifies this definition and states the general relation between conjugate pairs of discrete minimal surfaces.

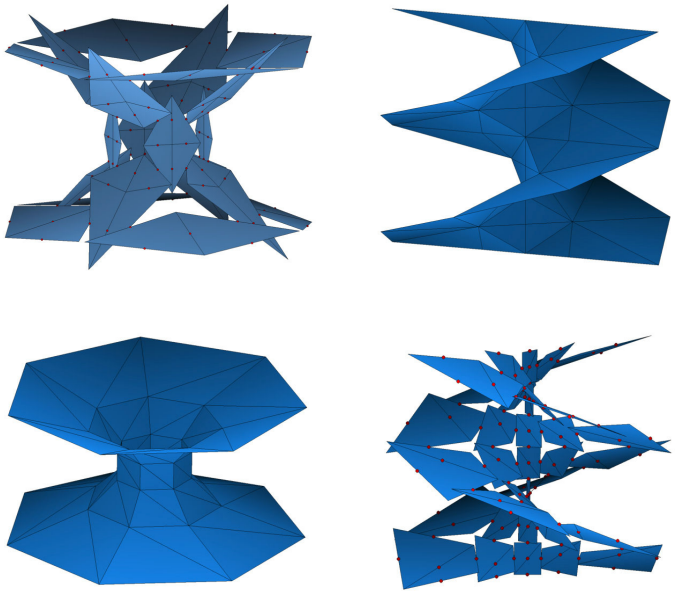

FIGURE 3.3. Pairs of conforming and non-conforming catenoids and helicoids where horizontal pairs are discrete conjugate.

Theorem 60 *1. Let $M_h \subset \mathbb{R}^d$ be a discrete minimal surface in S_h. Then there exists a conjugate surface $M_h^* \subset \mathbb{R}^d$ in S_h^* which is critical for the area functional in S_h^*.*

2. Let $M_h \subset \mathbb{R}^d$ be a discrete minimal surface in S_h^*. Then there exists a conjugate surface $M_h^* \subset \mathbb{R}^d$ in S_h which is critical for the area functional in S_h.

3. M_h^* is uniquely determined by M_h up to translation.

4. M_h and M_h^* are isometric and have the same Gauss map in the sense that corresponding triangles are congruent and parallel.

5. Applying the conjugation twice leads to

$$M_h^{**} = -M_h$$

for a suitably chosen origin.

Proof. Since M_h is a critical for the area functional the identity map

$$\mathrm{id} : M_h \to M_h$$

is a discrete harmonic map by Corollary 52. Therefore, Theorem 37 in Section 2 proves that there exist conjugate harmonic component

functions which give rise to a map on M_h

$$\mathrm{id}^* : M_h \to \mathbb{R}^d.$$

with $M_h^* := \mathrm{id}^* M_h$.

It remains to show that M_h^* is a discrete minimal surface. Here we assume that M_h is in S_h - the case M_h in S_h^* would work with the same words.

We show that M_h^* fulfills the balancing condition. Let $p^* \in M_h^*$ be an interior vertex, then by harmonicity of $\mathrm{id}^* \in S_h^*$ we have

$$\begin{aligned} \frac{d}{dm^*} E_D(\mathrm{id}^*) &= 2(\cot\alpha_{-2}(m^* - m_{-1}^*) + \cot\alpha_{-1}(m^* - m_0^*) \\ &\quad + \cot\alpha_1(m^* - m_2^*) + \cot\alpha_2(m^* - m_1^*)) \\ &= 0 \end{aligned} \tag{3.15}$$

where m^* and m_i^* are the images of id^* of edge midpoints in M_h.

Since on each triangle id^* is a rotation by $\frac{\pi}{2}$, corresponding triangles of M_h and M_h^* are isometric and have the same angles. Therefore, Equation 3.15 also is the criticality condition of the Dirichlet energy of the identity map of M_h^* which lies in S_h^*. Thus M_h^* is a discrete minimal surface in S_h^*.

The uniqueness follows from the uniqueness of the conjugate harmonic map and its integration constants. □

Summarizing, the theorem shows that a conjugate pair of discrete minimal surfaces does not exist in the space of piecewise linear conforming elements S_h but naturally leads to the space of piecewise linear non-conforming Crouzeix-Raviart elements S_h^*. S_h alone is too rigid to contain the conjugate of a minimal surface too.

In other words, if M_h is be a simplicial minimal surface in S_h respectively in S_h^* then its discrete conjugate minimal surface M_h^* is the image of the conjugate harmonic $\mathrm{id}^* : M_h \to \mathbb{R}^d$ map of the identity map of $\mathrm{id} : M_h \to M_h$, that is, id and id^* fulfill

$$d\,\mathrm{id}^* = *d\,\mathrm{id}\,.$$

The usage of the same domain M_h for both identity maps seems to distinguish M_h from M_h^* but only the conformal structure of the domain surface is relevant for the minimality condition. Therefore, we may instead use M_h^* or, more appropriate, use $\mathrm{id} : M_h \to M_h$ and $\mathrm{id}^* : M_h^* \to M_h^*$.

3.6.2 Numerical Conjugation

In practical applications the conjugation of a simplicial minimal surface by rotating each triangle and reassembling the rotated copies requires that the simplicial minimal surface has been computed very exact. Often, minimal surfaces are computed by solving a variational problem where the numerical method stops before reaching the absolute zero of the gradient. A much more stable procedure has been suggested in [25] to circumvent this difficulty: in a minimization procedure based on the Dirichlet energy there exists an accurately computed harmonic map F_i between the last two compute surfaces M_i and M_{i-1}. Instead of by applying the conjugation to the approximation M_i of the limit minimal surface, it is more stable to compute the harmonic conjugate map

$$F_i^* : M_{i-1} \to M_i^*.$$

The following algorithm summarizes the procedure:

Algorithm 61 *To compute the conjugate M_h^* of the Plateau problem M_h with Dirichlet boundary condition Γ:*

1. Follow the minimization algorithm above to compute a sequence of discrete harmonic maps $F_i : M_i \to M_{i+1}$.
2. Compute the harmonic conjugate F_i^* of $F_i : M_i \to M_{i+1}$.
3. Set $M_h := M_{i+1}$ as numerical approximation of the Plateau solution, and set $M_h^* := F_i^*(M_i)$ as approximation of the conjugate minimal surface.

This algorithm generates a sequence of discrete surfaces $\{M_i\}$ and vector-valued harmonic maps $\{F_i : M_i \to M_{i+1}\}$ which converges to a minimal surface if no degeneration occurs. In order to extend the conjugation technique of the previous sections to the computation of the conjugate of a minimal surface we allow the surfaces M_i to be either all conforming or all non-conforming triangulations. In this case the coordinate functions of each F_i are discrete harmonic functions either in S_h or S_h^*, and the image $F_i^*(M_i)$ of the conjugate harmonic of F_i is a good approximation of the conjugate minimal surface. The two approximations M_h and M_h^* are either a conforming and a non-conforming triangulation, or vice-versa.

Remark 62 *The output of the numerical conjugation algorithm 61 is a conforming mesh if one uses a non-conforming triangulation to*

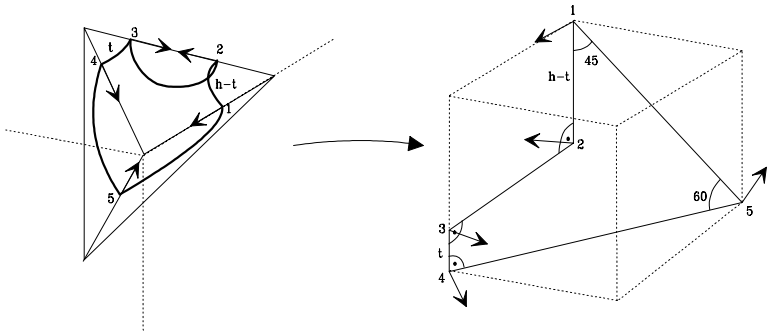

FIGURE 3.4. Transformation of a free-boundary value problem into a family of Dirichlet boundary value problems with a fixed contour.

solve the Dirichlet boundary conditions. The resulting stability problems when minimizing the non-conforming mesh are solved in [28].

3.7 Discrete Minimal Catenoid

Examples are important building blocks in the development of a mathematical theory. The first smooth minimal surfaces were found already in the 18th century when Lagrange formulated the variational characterization of minimal surfaces. The French geometer and engineer Jean Baptiste Meusnier (1754-1793) recognized the first nontrivial examples of minimal surfaces: the catenoid found by Euler in 1744, also called the chain surface, because it is the surface swept out when one rotates the catenary curve that corresponds to a freely hanging chain about a suitable horizontal line, and the helicoid, or screw surface. Already the discovery of the next examples in 1835 was regarded as so sensational that its discoverer Heinrich Ferdinand Scherk (1798-1885), Professor at Kiel and Bremen, won a prize at the Jablonowski Society at Leipzig in 1831.

The discovery of this discrete minimal catenoid by Polthier and Rossman [32] was driven by a very practical need, namely the provision of an unstable discrete minimal surface for investigations on the index of minimal surfaces. The numerical eigenvalue computations require a very accurate unstable surface as input which is hardly produced by means of minimization methods. Here the explicit formulae allows us to create unstable catenoids of arbitrary resolution. The model [29] at the EG-Models journal includes an interactive applet to study the whole family of discrete catenoids.

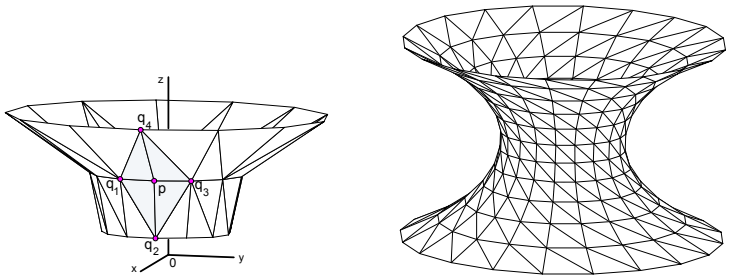

FIGURE 3.5. Discrete catenoid with essential stencil.

The strategy for the construction of an explicit formula for embedded complete discrete minimal catenoids is to assume that the vertices lie on congruent planar polygonal meridians and that the meridians placed so that the traces of the surfaces will have dihedral symmetry. Under these assumptions we find that the vertices of a discrete meridian lie equally spaced on a smooth hyperbolic cosine curve. Furthermore, these discrete catenoids will converge uniformly in compact regions to the smooth catenoid as the mesh is made finer.

We now state an explicit formula for discrete minimal catenoids, by specifying the vertices along a planar polygonal meridian. Then the traces of the surfaces will have dihedral symmetry of order $k \geq 3$. The surfaces are tessellated by planar isosceles trapezoids like a $\mathbb{Z}^2$ grid, and each trapezoid can be triangulated into two triangles by choosing a diagonal of the trapezoid as the interior edge. Either diagonal can be chosen, as this does not affect the minimality of the catenoid.

The discrete catenoid has two surprising features. First, the vertices of a meridian lie on a scaled smooth cosh curve (just as the profile curve of smooth catenoids lies on the cosh curve), and there is no apriori reason to have expected this. Secondly, the vertical spacing of the vertices along the meridians is constant.

Theorem 63 (joint with W. Rossman) *There exists a four-parameter family of embedded and complete discrete minimal catenoids $C = C(\theta, \delta, r, z_0)$ with dihedral rotational symmetry and planar meridians. If we assume that the dihedral symmetry axis is the z-axis and that a meridian lies in the xz-plane, then, up to vertical translation, the catenoid is completely described by the following properties:*

1. *The dihedral angle is $\theta = \frac{2\pi}{k}$, $k \in \mathbb{N}$, $k \geq 3$.*

2. *The vertices of the meridian in the xz-plane interpolate the smooth* cosh *curve*

$$x(z) = r\cosh\left(\frac{1}{r}az\right),$$

with

$$a = \frac{r}{\delta}\operatorname{arccosh}\left(1 + \frac{1}{r^2}\frac{\delta^2}{1+\cos\theta}\right),$$

where the parameter $r > 0$ is the waist radius of the interpolated cosh *curve, and $\delta > 0$ is the constant vertical distance between adjacent vertices of the meridian.*

3. *For any given arbitrary initial value $z_0 \in \mathbb{R}$, the profile curve has vertices of the form $(x_j, 0, z_j)$ with*

$$\begin{aligned} z_j &= z_0 + j\delta \\ x_j &= x(z_j) \end{aligned}$$

where $x(z)$ is the meridian in item 2 above.

4. *The planar trapezoids of the catenoid may be triangulated independently of each other.*

Corollary 64 *There exists a two-parameter family of discrete catenoids $C_1(\theta, z_0)$ whose vertices interpolate the smooth minimal catenoid with meridian $x = \cosh z$.*

Proof. The waist radius of the scaled cosh curve must be $r = 1$. Further, we must choose the parameter $a = 1$ which is fulfilled if θ and δ are related by $1 + \cos\theta + \delta^2 = (1 + \cos\theta)\cosh\delta$. The offset parameter z_0 may be chosen arbitrarily leading to a vertical shift of the vertices along the smooth catenoid. Note that if $z_0 = 0$, we obtain a discrete catenoid that is symmetric with respect to a horizontal reflection. □

Corollary 65 *For each fixed r and z_0, the profile curves of the discrete catenoids $C(\theta, \delta, r, z_0)$ approach the profile curve $x = r\cosh\frac{z}{r}$ of a smooth catenoid uniformly in compact sets of $\mathbb{R}^3$ as $\delta, \theta \to 0$.*

Proof. This is a direct consequence of the explicit representation of the meridian. Since

$$\lim_{\delta\to 0}\frac{1}{\delta}\operatorname{arccosh}(1 + \frac{1}{r^2}\frac{\delta^2}{1+\cos\theta}) = \frac{\sqrt{2}}{r\sqrt{1+\cos\theta}},$$

it follows that the profile curve of the discrete catenoid converges uniformly to the curve

$$x = r\cosh\frac{\sqrt{2}z}{r\sqrt{1+\cos\theta}}$$

as $\delta \to 0$. Then, as $\theta \to 0$ we approach the profile curve $x = r\cosh\frac{z}{r}$. □

3.8 Discrete Minimal Helicoid

We continue with the derivation of explicit discrete helicoids which are a natural second example of a complete, embedded discrete minimal surface. The full construction of the surface is given in [32]. An interactive data set of the model is available at the EG-Models site at [31].

In the smooth setting, there exists an isometric deformation through conjugate surfaces from the catenoid to the helicoid (see, for example, [24]). So, one might first try to make a similar deformation from the discrete catenoids in Theorem 63 to discrete minimal helicoids. But such a deformation is impossible in the space of edge-continuous triangulations. In fact, in order to make an associate family of discrete minimal surfaces, one must allow non-continuous triangle nets having greater flexibility.

Therefore, we adopt a different approach for finding discrete minimal helicoids. The helicoids will be comprised of planar quadrilaterals, each triangulated by four coplanar triangles, see Figures 3.5 and 3.3. Each quadrilateral is the star of a unique vertex, and none of its four boundary edges are vertical or horizontal, and one pair of opposite vertices in its boundary have the same z-coordinate, and the four boundary edges consist of two pairs of adjacent edges so that within each pair the adjacent edges are of equal length.

Theorem 66 (joint with W. Rossman) *There exists a family of complete embedded discrete minimal helicoids, with the connectivity as shown in Figure 3.5. The vertices, indexed by $i, j \in \mathbb{Z}$, are the points*

$$\frac{r\sinh(x_0 + j\delta)}{\sin\theta}(\cos(i\theta), \sin(i\theta), 0) + (0, 0, ir)\ ,$$

for any given real numbers $\theta \in (0, \frac{\pi}{2})$ and $r, \delta \in \mathbb{R}$.

Note that these surfaces are invariant under the screw motion that combines vertical upward translation of distance $2r$ with rotation about the x_3-axis by an angle of 2θ. The term x_0 determines the offset of the vertices from the $z-$axis (if $x_0 = 0$, then the z-axis is included in the edge set), and δ determines the horizontal spacing of the vertices. The homothety factor is r, which equals the vertical distance between consecutive horizontal lines of edges.

References

[1] A. D. Aleksandrov and V. A. Zalgaller. *Intrinsic Geometry of Surfaces*, volume 15 of *Translation of Mathematical Monographs*. AMS, 1967.

[2] E. D. Bloch. *A First Course in Geometric Topology and Differential Geometry*. Birkhäuser Verlag, 1997.

[3] K. Brakke. *Surface Evolver Manual v2.14*, 1999. http://www.susqu.edu/facstaff/b/brakke/evolver.

[4] S. C. Brenner and L. R. Scott. *The Mathematical Theory of Finite Element Methods*. Springer Verlag, 1994.

[5] P. Ciarlet. *The Finite Element Method for Elliptic Problems*. North-Holland, 1978.

[6] U. Dierkes, S. Hildebrandt, A. Küster, and O. Wohlrab. *Minimal Surfaces*, volume 1 of *Grundlehren der Mathematik*. Springer Verlag, 1992.

[7] G. Dziuk. An algorithm for evolutionary surfaces. *Numer. Math.*, 58:603–611, 1991.

[8] G. Dziuk and J. E. Hutchinson. Finite element approximations and the Dirichlet problem for surfaces of prescribed mean cur-

vature. In H.-C. Hege and K. Polthier, editors, *Mathematical Visualization*, pages 73–87. Springer-Verlag, Heidelberg, 1998.

[9] M. S. Floater. Parametrization and smooth approximation of surface triangulations. *Computer Aided Geometric Design*, 14:231–250, 1997.

[10] M. Gromov. *Metric structures for Riemannian and non-Riemannian spaces*, volume 152 of *Progress in Mathematics*. Springer-Verlag, 1999.

[11] I. Guskov, K. Vidimce, W. Sweldens, and P. Schröder. Normal meshes. In *Computer Graphics Proceedings (Siggraph '00)*, pages 95–102, 2000.

[12] H. Hoppe. Progressive meshes. *Computer Graphics (SIGGRAPH '96 Proceedings)*, pages 99–108, August 1996.

[13] L. Hsu, R. Kusner, and J. Sullivan. Minimizing the squared mean curvature integral for surfaces in space forms. *Experimental Mathematics*, 1(3):191–207, 1992.

[14] K. Hurdal, P. L. Bowers, K. Stephenson, D. W. L. Sumners, K. Rehm, K. Schaper, and D. A. Rottenberg. Quasi-conformally flat mapping the human cerebellum. In C. Taylor and A. Colchester, editors, *Medical Image Computing and Computer-Assisted Intervention - MICCAI'99*, volume 1679 of *Lecture Notes in Computer Science*, pages 279–286. Springer Verlag, 1999.

[15] J. E. Hutchinson. Computing conformal maps and minimal surfaces. *Proc. Centr. Math. Anal., Canberra*, 26:140–161, 1991.

[16] H. L. Jr. *Lectures on Minimal Submanifolds*. Publish or Perish Press, 1971.

[17] H. Karcher. Construction of minimal surfaces. *Surveys in Geometry, University of Tokyo*, pages 1–96, 1989.

[18] H. Karcher and K. Polthier. Construction of triply periodic minimal surfaces. In J. Klinowski and A. L. Mackay, editors, *Curved Surfaces in Chemical Structures*, volume 354 (1715) of *A*, pages 2077–2104. The Royal Society, London, Great Britain, phil. trans. r. soc. lond. edition, September 1996.

[19] Z. Karni and C. Gotsman. Spectral compression of mesh geometry. In *Computer Graphics Proceedings (Siggraph '00)*, pages 279–286. ACM SIGGRAPH, 2000.

[20] E. E. Moise. *Geometric Topology in Dimensions 2 and 3.* Springer Verlag, 1977.

[21] S. Müller, M. Struwe, and V. Sverak. Harmonic maps on planar lattices. Technical Report 17, MPI Leipzig, 1997.

[22] J. R. Munkres. *Elements of Algebraic Topology.* Addison Wesley, 1984.

[23] B. Oberknapp and K. Polthier. An algorithm for discrete constant mean curvature surfaces. In H.-C. Hege and K. Polthier, editors, *Visualization and Mathematics*, pages 141–161. Springer Verlag, Heidelberg, 1997.

[24] R. Osserman. *A Survey of Minimal Surfaces.* Dover, 1986.

[25] U. Pinkall and K. Polthier. Computing discrete minimal surfaces and their conjugates. *Experim. Math.*, 2(1):15–36, 1993.

[26] E. Polak. *Computational Methods in Optimization.* Academic Press, 1971.

[27] K. Polthier. Polyhedral surfaces of constant mean curvature. Habilitationsschrift, Technische Universität Berlin, 2002.

[28] K. Polthier. Unstable periodic discrete minimal surfaces. In S. Hildebrandt and H. Karcher, editors, *Nonlinear Partial Differential Equations*, pages 127–143. Springer Verlag, 2002.

[29] K. Polthier and W. Rossman. Discrete catenoid. *Electronic Geometry Models*, 2000. http://www.eg-models.de/2000.05.002/.

[30] K. Polthier and W. Rossman. Counterexample to the maximum principle for discrete minimal surfaces. *Electronic Geometry Models*, 2001. http://www.eg-models.de/2000.11.040/.

[31] K. Polthier and W. Rossman. Discrete minimal helicoid. *Electronic Geometry Models*, 2001. http://www.eg-models.de/2001.01.046/.

[32] K. Polthier and W. Rossman. Discrete constant mean curvature surfaces and their index. *J. reine angew. Math*, 549(47–77), 2002.

[33] K. Polthier and M. Schmies. Straightest geodesics on polyhedral surfaces. In H.-C. Hege and K. Polthier, editors, *Mathematical Visualization*, pages 135–150. Springer Verlag, Heidelberg, 1998.

[34] W. H. Press, S. A. Teukolsky, W. T. Vetterling, and B. P. Flannery. *Numerical Recipies in C: The Art of Scientific Computing*. Cambridge University Press, 1993. `http://www.nr.com/`.

[35] Y. G. Reshetnyak. *Geometry IV*, volume 70 of *Encyclopaedia of Mathematical Sciences*, chapter 1. Two-Dimensional Manifolds of Bounded Curvature, pages 3–164. Springer Verlag, 1993.

[36] G. Taubin and J. Rossignac. Geometric compression through topological surgery. *ACM Transactions on Graphics*, 17(2):84–115, 1998.

[37] T. Tsuchiya. Discrete solutions of the Plateau problem and its convergence. *Math. of Comp.*, 49:157–165, 1987.

[38] G. M. Ziegler. *Lectures on Polytopes*. Springer Verlag, 1998. 2nd ed.